Chemical Geology 285 (2011) 215–230

Contents lists available at ScienceDirect

Chemical Geology

journal homepage: www.elsevier.com/locate/chemgeo

Hydrological control of stream water chemistry in a glacial catchment (Damma Glacier, Switzerland)

Ruth S. Hindshaw [a,b,*], Edward T. Tipper [c], Ben C. Reynolds [a], Emmanuel Lemarchand [a,b], Jan G. Wiederhold [a,b], Jan Magnusson [d], Stefano M. Bernasconi [e], Ruben Kretzschmar [b], Bernard Bourdon [a,1]

[a] Institute of Geochemistry and Petrology, ETH Zurich, Clausiusstrasse 25, 8092 Zurich, Switzerland
[b] Institute of Biogeochemistry and Pollutant Dynamics, ETH Zurich, CHN, Universitätstrasse 16, 8092 Zurich, Switzerland
[c] Department of Earth Sciences, University of Cambridge, Downing Street, Cambridge, CB2 3EQ, United Kingdom
[d] WSL Institute for Snow and Avalanche Research SLF, Flüelastrasse 11, 7260 Davos Dorf, Switzerland
[e] Geological Institute, ETH Zurich, Sonneggstrasse 5, 8092 Zurich, Switzerland

ARTICLE INFO

Article history:
Received 15 February 2011
Received in revised form 4 April 2011
Accepted 16 April 2011
Available online 27 April 2011

Editor: J.D. Blum

Keywords:
Glacial weathering
Hydrogeochemistry
Damma glacier
Strontium isotopes
Oxygen isotopes
Granite weathering

ABSTRACT

The temporal and spatial controls of stream water chemistry in a small, granitic, glacial catchment were investigated in conjunction with high-resolution hydrological and meteorological measurements. Significant systematic seasonal and diurnal variations were observed in the stream water chemistry, which were not caused by the mixing of water draining different lithologies. A hydrological model (ALPINE3D, Lehning et al., 2006) was used to calculate the relative contributions of the principal water sources, snow melt and ice melt, throughout the period of this study. Pronounced seasonal minima in $\delta^{18}O$ and $^{87}Sr/^{86}Sr$ were attributed to spring snow melt. Clear changes in X/Si ratios (X = Ca, Mg, K, Na, Sr) between summer and winter were observed. These changes are interpreted to reflect seasonal changes in the average residence time of water in the sub-glacial drainage network with short residence times in summer, when the discharge was greatest, leading to high X/Si ratios, and long residence times in winter, when the discharge was lowest, resulting in low X/Si ratios. This study shows that the time dependent stoichiometry of cation to Si ratios in glacial stream water (and likely all catchments) strongly depends on the hydrological state of the catchment at the time of sampling. Annual fluxes based on spot samples varied by a factor of six depending on the time of year in which the sample was collected, highlighting the importance of long-term catchment monitoring. An improved understanding of the spatial and temporal controls acting on stream water chemistry will allow silicate weathering processes to be more precisely quantified.

1. Introduction

Globally, the chemical composition of river water varies widely (Meybeck, 2003). Although much of this variation can be attributed to different lithologies (Reeder et al., 1972; Gaillardet et al., 1999), there is considerable variation between rivers draining similar lithologies (Gíslason et al., 1996; White et al., 1999; Oliva et al., 2003). The relative importance of the different extrinsic weathering factors such as climate, runoff, tectonics and vegetation on runoff composition is still debated (Bluth and Kump, 1994; White and Blum, 1995; Oliva et al., 2003; Riebe et al., 2004; West et al., 2005) and disentangling these factors is difficult since they are not independent variables, e.g. temperature affects runoff and local vegetation. The majority of studies that have derived estimates of CO_2 consumption by silicate weathering, based on river chemistry, have assumed that the chemical composition of a single river derived from spot sampling is invariant. However, an increasing number of studies of large rivers indicate significant seasonal variations in chemical composition (Cameron et al., 1995; Yang et al., 1996; Shiller, 1997; Galy and France-Lanord, 1999; France-Lanord et al., 2003; Zakharova et al., 2005; Tipper et al., 2006; Ollivier et al., 2010) and long term studies highlight the inter-annual variability of annual weathering fluxes (Likens et al., 1998; Gupta et al., 2011). Time series data are vital in order to obtain accurate annual chemical weathering fluxes but also offer an unrivalled opportunity to understand the underlying mineral weathering processes. This is because lithology, the major control of stream water chemistry, is constant whilst external variables such as climate and hydrology vary, permitting an assessment of these variables on chemical weathering processes.

High frequency sampling studies of rivers to investigate temporal variability have tended to focus on alpine catchments which are either glaciated (Fairchild et al., 1999; Hodson et al., 2000; Mitchell et al., 2001; Hosein et al., 2004) or snow covered (e.g. Marsh and Pomeroy,

* Corresponding author.
E-mail address: hindshaw@erdw.ethz.ch (R.S. Hindshaw).
[1] Laboratoire des Sciences des la Terre, ENS Lyon, 46 Allée d'Italie, F-69364 Lyon.

0009-2541/$ – see front matter © 2011 Elsevier B.V. All rights reserved.
doi:10.1016/j.chemgeo.2011.04.012

1999). The bias towards alpine catchments results from these catchments' importance in hydroelectric power and summer water supply (Viviroli and Weingartner, 2004). Consequently, the focus of many of these studies has been to ascertain where the *water* comes from and not where the *solutes* originated (Malard et al., 1999). As a result, the hydrology of glacial catchments tends to be very well understood making them an ideal choice for gaining a better understanding of chemical weathering processes.

Combining the hydrological approaches (e.g. hydrograph separation Buttle, 1994) with the chemical approaches (e.g. mass balance Garrels and Mackenzie, 1967) offers a unique opportunity to improve our understanding of the processes which control stream water chemistry. A number of studies have used such a combination, most notably that of Clow and Drever (1996) who artificially enhanced discharge and studied the resultant effects, proving that discharge has an important control over solute acquisition. Other studies have found the role of discharge to be less important, invoking chemostatic behaviour (Godsey et al., 2009; Clow and Mast, 2010). These studies strongly indicate that although the weathering of primary minerals provides solutes, it is the secondary processes such as adsorption (Berner et al., 1998) and secondary mineral formation which actually control the resultant chemical composition of the stream. These processes are not constant over the year (Clow and Mast, 2010) and are very difficult to constrain. More data is needed to assess their relative importance.

Glacial catchments are ideal for exploring and further constraining the controls on stream water chemistry. Due to the large fluctuations in discharge over diurnal and seasonal timescales, the role of discharge in changing stream water chemical compositions can be evaluated. In addition, the changes in glacier hydrology over the season and the development of glacial drainage systems are relatively well documented (e.g. Brown, 2002). Glacial studies are typically only conducted during the melt season, consequently, potential chemical changes from summer to winter are not well known. Additionally, the role of glaciers in enhancing or suppressing chemical weathering rates is still contested (Sharp et al., 1995; Anderson et al., 1997).

Studies which use the dissolved load composition in order to understand weathering reactions often have weak links to catchment hydrology. In this study, we investigate whether hydrological source information can be used to explain the observed daily and seasonal changes occurring in glacial stream water chemistry in a small, granitic, alpine catchment by utilising major element, $^{87}Sr/^{86}Sr$ and $\delta^{18}O$ data. Identifying the main controls of solute acquisition will improve the quantification of weathering rates in catchments where discharge data is available but frequent chemical sampling is not possible.

2. Study area

The study area was the Damma glacier forefield: a small (10.7 km^2), granitic catchment situated in the central Swiss Alps, which is currently being studied as part of the BigLink project (Bernasconi et al., 2008). The glacier covers 40% of the catchment and has been retreating since ~1850 (VAW, 2005). Due to a sharp change in gradient a small piece (~0.14 km^2) of glacier has become detached from the main glacier during retreat and is referred to as 'dead ice'. Large side moraines are present dating from approximately 1850 (the end of the Little Ice Age) and two terminal moraine bands dating from 1927 and 1992 mark the end of two short periods of re-advance (VAW, 2005). The elevation of the catchment ranges from 1800 m to 3300 m and the entire catchment is snow covered for approximately 6 months of the year. The average annual temperature is 2.2 °C, annual precipitation is ~2300 mm and annual runoff is ~2700 mm. Evapotranspiration was estimated to be 70 mm in 2008 (Kormann, 2009). The positive water balance is due to the negative mass balance of the glacier.

The valley floor is a braided stream system, and the streams are ephemeral. The main stream, the Dammareuss, passes underneath the dead ice whilst the side stream cuts through the western side moraine (Fig. 1). A gauging station has been installed downstream of the confluence between the side and the main stream and at the confluence the side stream contributes approximately one third of the discharge.

The catchment is underlain by the central Aar granite which has an intrusion age of 298 Ma (Schaltegger, 1994), though further metamorphic resetting took place around 50 Ma (Dempster, 1986). The average mineralogy is: quartz (32%), plagioclase (32%, $An_{0.1}$), microcline (23%), muscovite (6%), biotite (4%), epidote (3%) together with trace amounts of apatite. Biotite was extensively altered to chlorite during Alpine orogeny (Dempster, 1986). Negligible levels of carbonate (91 ± 83 mg/kg, $1\sigma_{SD}$) were detected by coulometric titration in the rock samples which have been analysed so far (de Souza et al., 2010). The soils in the glacier forefield are thin, weakly developed and often contain large rock fragments.

3. Sampling and analytical methods

Water sampling was conducted at fortnightly intervals during the summer of 2008, from 13th May to 28th October. In addition, two winter samples were collected on 16th January and on 8th April 2009. Three locations were sampled in order to assess spatial variability. The following provides a brief description of the sampling sites: Site E was the stream exiting from under the dead ice, Site B was the side stream where it incised the western side moraine and Site A was by the gauging station (Fig. 1), by which point above-ground braiding had

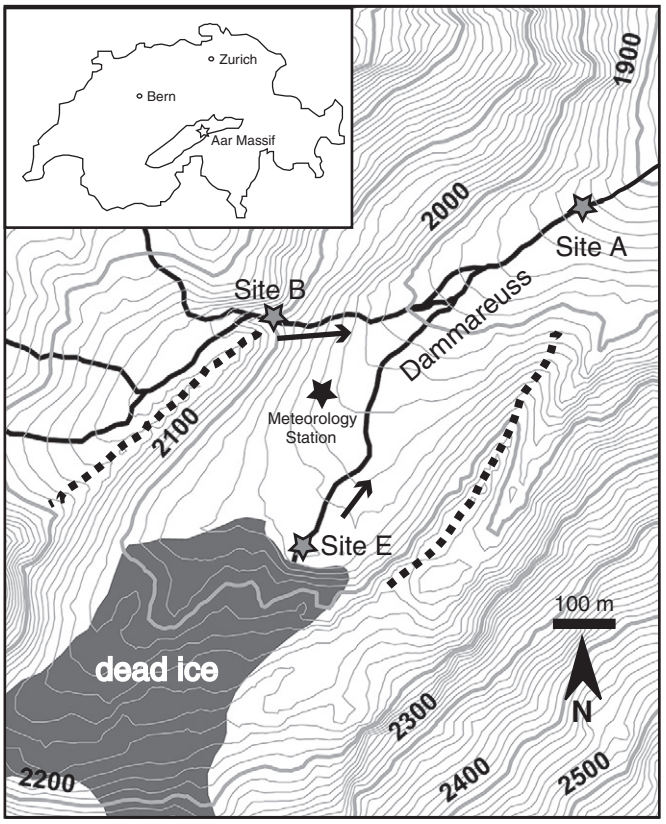

Fig. 1. Map of the sampling locations. Stars mark the stream water sampling locations and the meteorology station. Sites A and E lie on the main stream and Site B is on the side stream. The gauging station is situated at Site A. The side moraines, which date from 1850, are marked with dashed lines but the two most recent terminal moraines are not shown. Numbers indicate the height of the contour lines. The star in the inset shows the location of the Damma glacier in relation to the rest of Switzerland.

ceased. Two 24-hour sampling campaigns with hourly sampling were conducted on 24th–25th August 2008 and 2nd–3rd June 2009 at Site A. The gauging station recorded water discharge and conductivity every 10 min beginning early in the 2008 melt season (Fig. 2). The first two water samples were taken before the station was operational; for these samples the discharge was estimated. In addition to the gauging station, a meteorology station was erected in the middle of the forefield which recorded data every 30 min. Rainfall and temperature during the sampling period are shown in Fig. 2.

Rain water samples were collected using a 1.5 m high plastic cylinder located near the meteorology station. The cylinder had a plastic funnel at the top feeding into a 2 L plastic bottle and the top of the funnel was protected by a fine mesh to prevent insects from flying in. This bottle was emptied every two weeks. Although this method predominantly collected wet precipitation, a small amount of dry deposition may also have been collected if it was wind-blown into the funnel and subsequently dissolved. Snow samples were packed into pre-cleaned HDPE bottles wearing sterile gloves after removal of the top few centimetres of the snow pack and were allowed to melt naturally. Porewater samples were collected from suction cups installed at depths of 5–25 cm and groundwater samples were collected from tube wells which reached the water table.

All water samples were filtered in the field (snow samples were filtered once melted) using 0.2 μm nylon filters into pre-cleaned HDPE bottles. Bottles for cation analysis were cleaned using 2% HNO_3 and those for anion analysis were cleaned using MQ (Millipore) water. After filtration, samples for cation analysis were acidified to pH 2 with distilled HNO_3. A filtered water sample was titrated with 1.1 mM HCl and alkalinity was calculated from the titration curve using the Gran method (Stumm and Morgan, 1996).

Temperature and pH were recorded in situ (Hanna HI 98160 pH meter). Major cations (Ca^{2+}, Mg^{2+}, Na^{+}, K^{+}) and Si were measured by inductively-coupled plasma optical emission spectrometry (ICP-OES, Vista-MPX, Varian Inc., USA) and anions (Cl^{-}, F^{-}, NO_3^{-}, PO_4^{3-} SO_4^{2-}) were measured using ion chromatography (IC, 761 Compact IC, Metrohm AG, Switzerland). Phosphate in stream water samples was always below the detection limit of the IC (<50 ppb). Measured cation concentrations of the water standard SLRS-4 (National Research Council Canada) were within 10% of the certified values. Average relative standard deviations of repeat measurements of samples were: Na^{+} 12%, F^{-} 11%, K^{+} 9%, Ca^{2+} 8%, Si 7%, Cl^{-} 6%, Mg^{2+} and SO_4^{2-} 4%, and NO_3^{-} 3%. Calculated charge balance errors (CBE) were less than 2.5%, indicating the accuracy of the anion and cation measurements. Some higher charge balance errors were caused in winter samples by measuring the alkalinity back in the laboratory over 12 h after sample collection due to adverse weather conditions in the field. This could be due to oversaturation with respect to CO_2: degassing occurred, altering the carbonate equilibrium in the water sample, leading to an overestimation of [HCO_3^{-}] in the sample. This effect was also noted by Yde et al. (2005) and highlights the importance of immediate measurement in the field.

The oxygen isotopic composition was measured using the CO_2 equilibration method: 200 μL samples of water were pipetted into 12 mL septum-capped vials which were subsequently filled with a mixture of 0.3% CO_2 and He. After equilibration at 25 °C for at least 18 h the CO_2/He mixture was measured using a Gas Bench II (Thermo Scientific) connected to an isotope ratio mass spectrometer (Delta V plus, Thermo Scientific). Measurements were calibrated with the international standards SMOW, SLAP and GISP. The results are reported in the conventional delta notation with respect to VSMOW and sample standard deviation ($2\sigma_{SD}$) was less than 0.1‰.

Samples for strontium isotope analysis were first purified, based on methods by Deniel and Pin (2001) and de Souza et al. (2010), to remove matrix ions. The $^{87}Sr/^{86}Sr$ ratio was measured, for the majority of samples, on a multicollector ICP-MS (Nu Plasma, Nu Instruments, UK). Solutions (50 ppb) were introduced to the mass spectrometer using a PFA microconcentric nebuliser with an uptake rate of ~50 μL/min and the aerosol was dried using a desolvator (either Aridus II, Apex Q or Apex HF depending on the session). This gave a minimum ^{88}Sr ion beam intensity of 5×10^{-11} A. Krypton and Rb interferences were corrected using an on-peak zero and an iterative correction for any residual Kr and Rb above background (de Souza et al., 2010). The mass bias calculated for Sr was assumed to be valid for Rb and Kr. This is valid since the magnitude of this correction was small compared to the external reproducibility. Samples were bracketed by NBS 987 and all samples and standards were normalised to $^{86}Sr/^{88}Sr = 0.1194$. Due to a clear drift in the standard values a secondary correction to give NBS 987 $^{87}Sr/^{86}Sr$ ratios of 0.710250 was used. Each sample was measured at least twice. Reproducibility ($2\sigma_{SD}$) of standards over the course of this study were 0.709182 ± 66 and 0.708665 ± 59 for seawater and an in-house standard respectively. Sample standard deviation ($2\sigma_{SD}$) was less than 80 ppm. Samples not measured by ICP-MS were measured by thermal ionisation mass spectrometry (TIMS) (Triton, Thermo Fischer Scientific). Approximately 250 ng of Sr was loaded in nitric form together with

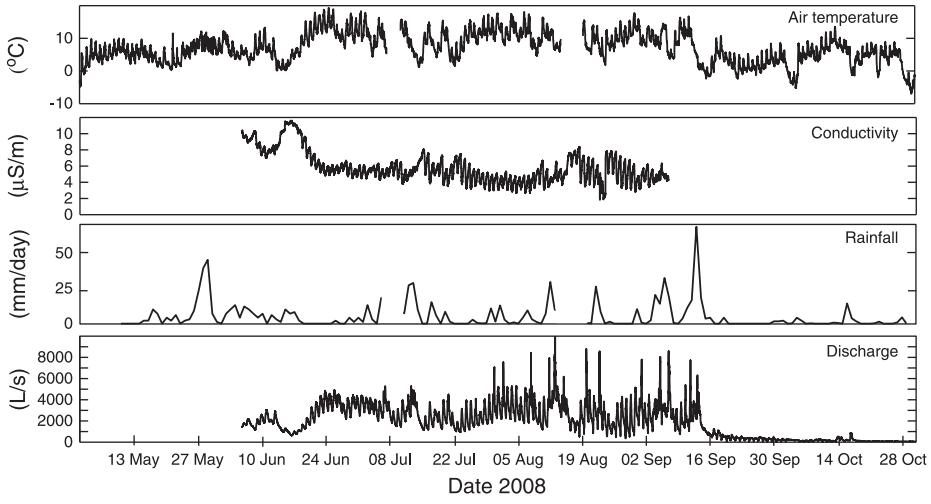

Fig. 2. Main parameters recorded at the gauging station and at the meteorology station during 2008. Conductivity is inversely related to discharge but does not react strongly to rainfall events which cause large, short-lived spikes in discharge. No data was recorded by the meteorology station from 7th–10th July and 14th–19th August due to technical problems.

1 μL of tantalum phosphate activator solution onto degassed single rhenium filaments. Data acquisition was comprised of 200 measurements with a 4 s integration time in static mode. The exponential law was applied to correct for instrument mass fractionation and all $^{87}Sr/^{86}Sr$ ratios were normalised to $^{86}Sr/^{88}Sr = 0.1194$. ^{85}Rb was monitored to correct for rubidium interferences on ^{87}Sr. At least two different standards (of NBS 987, seawater and an in-house standard) were analysed in each session to monitor machine drift and each sample was measured four times. Similar to ICP-MS, a secondary correction was applied to all data. Reproducibility ($2\sigma_{SD}$) of standards over the course of this study were 0.709181 ± 25 and 0.708669 ± 18 for seawater and the in-house standard respectively. Sample standard deviation ($2\sigma_{SD}$) was less than 40 ppm. Sample 20080624A was measured by both methods and yielded identical results of 0.720637 ± 36 (MC-ICP-MS) and 0.720636 ± 25 (TIMS).

4. Hydrology and water chemistry

4.1. Catchment meteorology and hydrology

Air temperature, conductivity, rainfall and discharge all showed significant temporal variability during 2008 (Fig. 2). As expected for a glacial catchment, discharge exhibited a strong seasonal trend with maximum discharge during the summer months and an abrupt cessation of flow coinciding with the first snow in autumn. Heavy rain events in the summer caused rapid increases in discharge with flows reaching in excess of 6000 L s^{-1}. Superimposed on the seasonal discharge trend were strong diurnal cycles linked to the melting of the glacier during the day. Conductivity was inversely related to discharge and exhibited diurnal and seasonal variations. The conductivity of the stream water was not strongly correlated with heavy rainfall events.

Pronounced seasonal and diurnal variations were observed in $\delta^{18}O$ which were similar in magnitude at all three sites (Fig. 3). Stream water sampled at the start of the melt season was depleted in ^{18}O ($\delta^{18}O \sim -17‰$) and as melting progressed the $\delta^{18}O$ value measured in the stream rapidly increased. From July onwards $\delta^{18}O$ continued to increase, but at a slower rate, until the winter months when no further increase in $\delta^{18}O$ was observed. The highest $\delta^{18}O$ values reached were around −14‰. Similar seasonal trends in $\delta^{18}O$ have been previously recorded in snow affected catchments (Bottomley et al., 1986; Taylor et al., 2001; Unnikrishna et al., 2002; Liu et al., 2004).

The diurnal amplitudes of $\delta^{18}O$ variation were 0.3‰ and 0.6‰ in June and August respectively, which were less than the seasonal amplitude of 3‰ (Tables 1 and 2). In June, $\delta^{18}O$ was inversely related to discharge but there was a significant phase shift with the minimum $\delta^{18}O$ value reached seven hours after maximum discharge. The diurnal minimum can be explained by increased melting in response to increased solar radiation during the day. The first half of the August $\delta^{18}O$ diurnal cycle was also inversely related to discharge, but the minimum $\delta^{18}O$ value was observed two hours before maximum discharge. In August a second minimum occurred during the night and this could have been caused by ice melt contributions at night due to high night-time air temperatures (Jobard and Dzikowski, 2006).

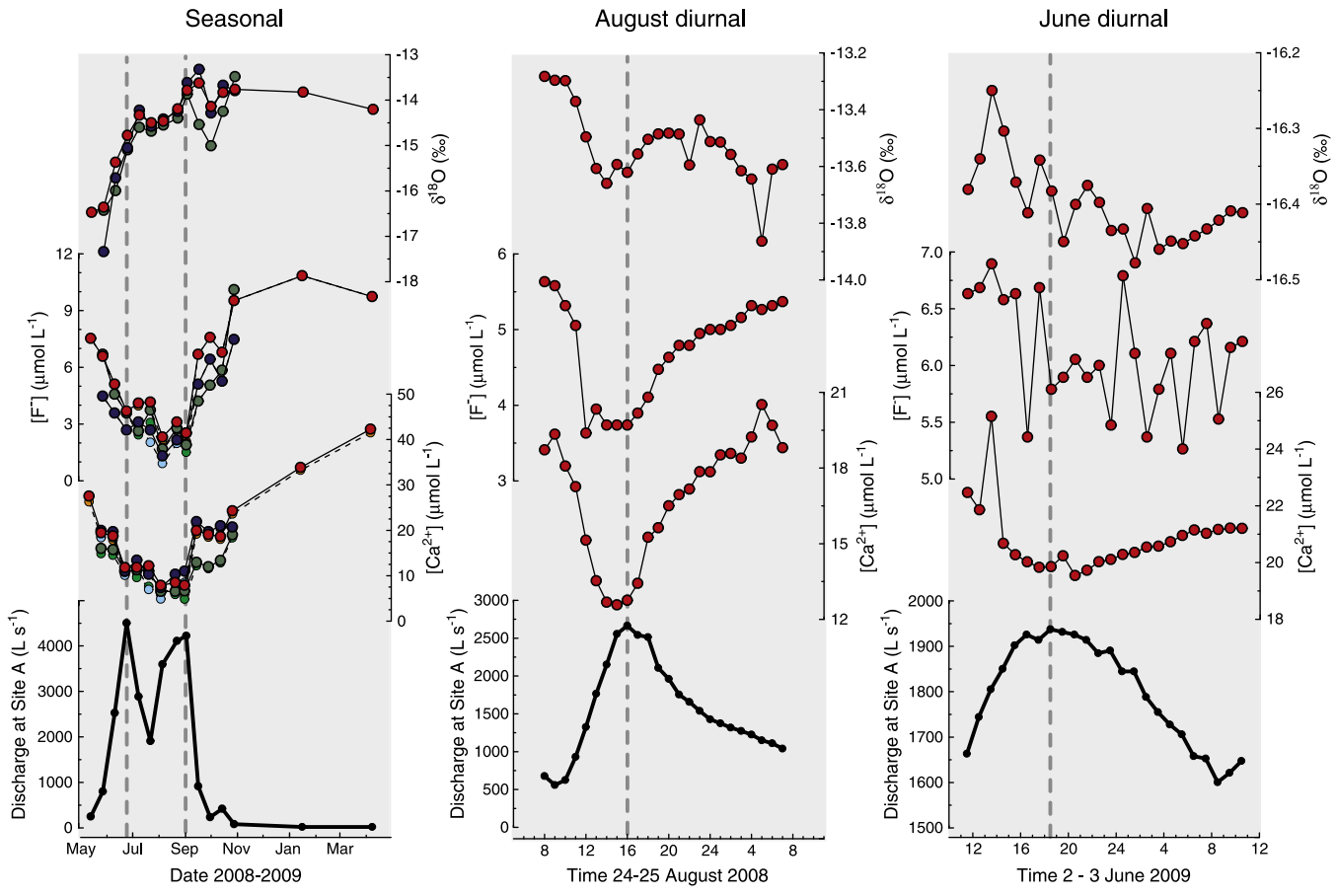

Fig. 3. Left column: Seasonal changes in discharge, cation concentrations (represented by Ca^{2+}), anion concentrations (represented by F^-) and $\delta^{18}O$. Red symbols are data from Site A, green symbols are for Site B and blue symbols are for Site E. Precipitation corrected values are indicated by orange, light green and light blue for Sites A, B and E respectively and are joined by a dashed line. For most data points the correction is too small to observe. Centre and right columns: Diurnal data for discharge, cation concentrations, anion concentrations and $\delta^{18}O$, from site A during August and June respectively. The vertical dashed lines indicate times of maximum discharge.

Table 1
Major species, $^{87}Sr/^{86}Sr$, and $\delta^{18}O$ data for seasonal sampling. R = rain and S = snow. Measurement reproducibility is described in the text.

Site	Date (YMD)	Time (CET)	Runoff ($L\,s^{-1}$)	pH	T (°C)	Ca^{2+}	Mg^{2+}	Na^{+}	K^{+}	Si ($\mu mol\,L^{-1}$)	F^{-}	Cl^{-}	NO_3^{-}	SO_4^{2-}	HCO_3^{-}	Sr^{2+} ($nmol\,L^{-1}$)	$\delta^{18}O$ (‰)	$^{87}Sr/^{86}Sr$
A	20080513	07:35	250	5.61	0.8	27.5	5.0	13.2	14.5	26.2	7.5	5.2	34.0	8.9	63.1	36.6	−16.47	0.72680
A	20080527	15:20	800	6.55	0.4	19.5	3.1	9.8	10.2	15.8	6.6	4.1	22.2	6.8		27.8	−16.36	0.72458
A	20080610	15:30	2528	6.34	4.7	18.7	3.3	8.9	9.5	14.6	5.1	3.6	15.8	5.9	26.2	28.3	−15.37	0.72070
A	20080624	15:30	4502	6.42	5.5	11.8	2.0	7.1	7.6	7.7	3.7	3.6	9.4	3.9	18.1	17.8	−14.78	0.72064
A	20080708	14:40	2886	6.23	6.3	11.8	2.1	6.3	7.9	9.9	4.1	3.0	9.1	4.0	16.6	18.1	−14.33	0.72194
A	20080722	15:30	1908	6.24	5.4	12.2	2.4	6.7	8.1	12.2	4.2	2.4	8.5	4.3	32.8	19.2	−14.50	0.72268
A	20080805	14:35	3595	6.51	10.5	7.9	1.5	4.3	5.5	6.4	2.3	1.9	5.2	2.5	13.9	12.3	−14.47	0.72310
A	20080819	15:35	4110	6.52	6.9	8.5	1.5	5.8	6.2	7.3	3.1	2.9	4.7	2.7	16.1	12.7	−14.19	0.72440
A	20080902	13:55	4221	6.15	5.9	7.9	1.4	3.3	4.7	6.1	2.5	1.9	4.8	2.6	13.4	11.7	−13.78	0.72486
A	20080916	15:30	916	5.84	4.9	19.9	4.1	13.9	16.1	30.0	6.7	3.2	14.5	9.1	40.6	36.1	−13.63	0.72278
A	20080930	17:00	236	5.75	4.2	19.1	4.5	15.5	16.1	37.6	7.6	2.5	12.7	7.9	49.6	34.0	−14.14	0.72319
A	20081014	14:30	420	5.55	4.2	18.6	3.6	12.4	13.2	24.1	6.8	2.5	16.6	7.9	33.6	34.7	−13.83	0.72320
A	20081028	09:50	84	5.75	2.6	24.3	5.5	24.3	20.3	54.3	9.5	3.0	14.7	10.3	97.5	42.7	−13.76	0.72489
A	20090116		20	6.30	2.2	33.9	7.8	29.8	24.0	71.1	10.8	2.6	15.7		80.4	48.2	−13.83	0.72370
A	20090408	08:05	20	6.05	2.5	42.3	11.1	35.7	24.9	70.6	9.7	3.3	40.9	14.3	72.6	73.7	−14.20	0.72445
B	20080527	13:50		6.37	−0.2	16.0	2.2	7.3	6.8	9.7	6.7	4.7	20.2	6.0		17.1	−16.43	0.73228
B	20080610	12:50		6.15	3.8	15.7	2.1	6.8	6.8	5.0	4.6	5.0	15.6	4.5	7.8	18.0	−15.99	0.72582
B	20080624	12:45		5.34	7.0	11.0	1.5	3.8	3.8	3.3	3.6	2.6	10.4	3.9	9.9	13.4	−15.10	0.72648
B	20080708	12:40		5.95	8.6	11.3	1.5	4.8	5.3	3.3	2.6	4.0	12.2	3.9	6.7	14.4	−14.60	0.72663
B	20080722	11:00	421	5.28	8.2	11.0	1.6	4.5	4.8	4.5	3.7	4.1	10.6	4.0	20.7	13.7	−14.69	0.72902
B	20080805	12:25	2092	6.43	8.4	6.5	0.9	1.7	2.4	2.0	1.7	1.0	4.4	1.8	5.8	7.7	−14.55	0.72975
B	20080819	13:00	2045	5.50	10.5	6.6	0.9	2.2	3.3	2.5	2.8	1.4	3.8	1.8	7.8	7.6	−14.40	0.73166
B	20080902	11:40	2078	5.97	7.4	6.7	0.9	2.2	3.6	2.6	1.9	1.7	4.7	2.0	6.0	7.8	−13.87	0.73248
B	20080916	13:10	175	5.88	6.7	12.9	1.7	4.7	4.9	7.3	4.2	3.0	14.5	5.8	16.6	17.6	−14.54	0.73140
B	20080930	12:15		5.90	4.5	12.0	1.6	4.7	5.5	12.3	5.1	1.7	19.6	3.8	12.8	15.1	−15.01	0.73095
B	20081014	12:10		4.90	6.1	13.4	1.8	6.0	6.4	11.2	5.8	2.2	19.0	6.0	12.0	19.0	−14.25	0.73083
B	20081028	10:20		7.30	3.5	19.0	3.0	16.0	11.0	39.3	10.1	2.8	15.9	6.6	69.8	24.3	−13.48	0.73018
E	20080527	09:30		5.83	0.2	20.0	2.9	8.9	10.0	9.4	4.5	6.5	28.9	8.4		38.6	−17.34	0.71875
E	20080610	09:30		6.40	1.3	19.7	3.7	9.3	11.3	10.3	3.6	5.4	17.8	6.8	30.6	37.7	−15.72	0.71570
E	20080624	09:15		7.19	2.5	11.0	2.1	6.6	8.6	6.4	2.7	3.6	10.7	3.9	17.1	20.3	−15.05	0.71712
E	20080708	09:10		7.15	2.0	13.4	2.7	7.1	9.3	10.3	3.1	3.4	12.0	5.0	22.1	24.1	−14.22	0.71761
E	20080722	14:00	892	6.10	2.0	10.3	2.2	6.9	8.2	7.9	2.7	4.1	7.8	3.8	28.1	20.1	−14.58	0.71820
E	20080805	09:00	1866	6.10	3.2	7.4	2.1	4.6	7.1	5.7	1.3	4.3	4.9	2.2	5.3	13.1	−14.42	0.71835
E	20080819	09:30	1083	6.20	3.1	10.3	2.1	5.7	–	8.9	2.2	2.6	6.1	3.9	20.4	19.5	−14.25	0.71889
E	20080902	08:40	723	5.98	2.5	11.0	2.2	5.3	7.8	8.1	2.5	2.4	7.5	4.5	17.1	22.6	−13.62	0.71892
E	20080916	09:45	230	6.58	1.1	21.9	5.3	13.9	17.9	26.9	5.1	2.7	17.1	12.2	50.8	50.9	−13.32	0.71831
E	20080930	09:30	50	6.16	1.2	19.7	4.9	14.0	17.7	31.9	6.4	2.9	17.3	8.9	46.4	40.9	−14.29	0.71946
E	20081014	09:00		6.45	1.5	21.0	3.8	10.9	14.4	19.3	5.3	2.2	20.8	9.0	37.8	45.7	−13.67	0.71938
E	20081028	12:40		5.85	1.3	20.7	5.4	16.2	19.6	35.2	7.5	2.2	20.5	10.8	54.7	45.2	−13.79	0.71990
R	20080624					4.6	0.5	2.3	2.0	2.4	0.0	4.9	22.4	5.4		2.8	−8.57	
R	20080708					12.7	1.4	2.7	2.3	1.6	0.0	4.7	20.8	6.9		13.5	−6.41	
R	20080726					5.2	0.6	2.5	2.2	1.6	0.0	3.0	12.4	3.8		3.7	−10.09	
R	20080805					7.8	1.2	4.2	2.5	0.1	0.0	5.8	23.2	8.0		10.3	−7.08	0.70933[a]
R	20080819					7.1	0.8	2.3	1.7	2.3	0.0	3.2	11.9	4.4		6.0	−8.55	
R	20080902					5.6	0.6	1.1	0.8	1.8	0.0	2.3	17.5	6.5		4.7	−7.40	
R	20080916					16.5	1.3	3.7	4.9	0.9	0.0	3.0	11.5	5.5		18.9	−10.54	
R	20080930					19.2	4.9	6.0	7.5	11.9	0.0	8.1	16.8	5.5		18.8	−13.96	0.70950[b]
S	20080513					2.2	0.1	1.7	0.7	0.05	0.0	6.4	4.9	1.0		1.7	−16.38	
S	20081028					6.2	0.4	4.0	1.8	0.00	0.0	21.0	15.5	3.2		2.9	−10.85	
S	20090116					3.8	0.2	1.4	8.8	0.00	0.0	20.4	8.8	3.2		1.8	−14.90	
S	20090116					1.8	0.2	2.0	2.3	0.01	0.0	6.7	6.9	1.7		1.6	−18.29	
S	20090116					2.7	0.4	3.8	3.3	0.00	0.0	7.4				2.9	−16.76	
S	20090406					4.9	0.8	26.6	7.6	0.11	0.4	29.9	9.8	2.2		6.4	−15.37	
S	20090407					2.5	0.2	0.9	1.6	0.13	0.0	9.3				1.1	−14.12	
S	20090407					0.6	0.1	0.4	0.6	0.09	0.0	4.0	6.1	0.6		0.5	−15.10	

PO_4^{3-} was measured but was below the detection limit.
[a] Average rain, first 4 samples of the season.
[b] Average rain, last 4 samples of the season.

4.2. Precipitation

There are three sources of precipitation inputs to the catchment to consider: rain, snow and indirectly ice, each of which has a different chemical and isotopic composition (Table 1, Tresch, 2007).

The $\delta^{18}O$ values for rain decreased from −7‰ in spring to −14‰ in late September. The decrease in $\delta^{18}O$ throughout the season is caused by changes in the precipitation source characteristics and air temperature (Gat, 1996; Unnikrishna et al., 2002). The chemical composition of the rain was variable and was dominated by Ca^{2+} and NO_3^{-}. The average $^{87}Sr/^{86}Sr$ of two composite rain samples was 0.70941 which is similar to the $^{87}Sr/^{86}Sr$ of rain recorded in a neighbouring catchment (Arn et al., 2003) and is considerably lower than the ratios measured in the stream waters (0.71570 to 0.73248, see Section 4.4).

The $\delta^{18}O$ values in snow were lower than for rain and were variable with time, depth and altitude[2], reflecting a heterogeneous snowpack (Unnikrishna et al., 2002). Snow samples were more dilute than rain samples and the dominant cation and anion was K^{+} or Ca^{2+} and Cl^{-} respectively. Si and F^{-} concentrations were negligible compared to those measured in the stream. A previous study in the

[2] The full $\delta^{18}O$ database can be found at http://www.cces.ethz.ch/projects/clench/BigLink.

Table 2
Major species, $^{87}Sr/^{86}Sr$ and $\delta^{18}O$ data for diurnal sampling. Measurement reproducibility is described in the text.

Time (CET)	Discharge (L s^{-1})	pH	T (°C)	Ca^{2+}	Mg^{2+}	Na^{+}	K^{+}	Si (μmol L^{-1})	F^{-}	Cl^{-}	NO_3^{-}	SO_4^{2-}	HCO_3^{-}	Sr^{2+} (nmol L^{-1})	$\delta^{18}O$ (‰)	$^{87}Sr/^{86}Sr$
24–25 August 2008																
08:00	677	5.78	3.7	18.7	3.7	10.5	13.2	20.5	5.6	2.7	11.6	7.2	29.2	28.2	−13.28	0.72289
09:00	559	5.52	4.7	19.3	3.8	10.9	12.5	22.0	5.6	2.5	11.6	7.7	32.4	29.5	−13.30	
10:00	625	5.61	5.3	18.1	3.5	9.8	11.9	19.0	5.3	2.1	11.5	7.3	31.1	26.9	−13.30	
11:00	931	5.52	6.0	17.3	3.3	9.4	11.4	17.6	5.1	1.9	10.5	6.6	27.8	26.5	−13.37	0.72229
12:00	1325	5.67	6.5	15.1	2.9	7.6	9.9	15.0	3.6	1.8	9.4	5.5	26.3	22.7	−13.50	
13:00	1766	5.61	6.8	13.5	2.6	6.7	8.8	13.2	3.9	1.6	8.2	4.8	22.1	20.5	−13.61	
14:00	2152	5.71	6.8	12.7	2.7	6.4	9.1	12.7	3.7	1.7	7.8	4.6	20.8	19.5	−13.66	0.72290
15:00	2557	5.73	6.6	12.6	2.3	5.8	7.9	11.4	3.7	1.5	7.5	4.3	19.9	19.0	−13.59	
16:00	2666	5.53	6.1	12.8	2.4	6.1	8.3	12.1	3.7	1.3	7.6	4.4	20.9	19.6	−13.62	
17:00	2542	5.55	5.5	13.4	2.5	6.4	8.2	12.6	3.9	1.2	8.0	4.8	23.9	20.7	−13.56	0.72324
18:00	2514	5.48	4.7	15.3	3.0	7.3	9.2	15.8	4.1	1.3	8.6	5.1	26.3	18.5	−13.50	
19:00	2108	5.70	4.6	15.6	3.0	8.0	9.7	16.7	4.5	1.4	9.0	5.5	26.2	23.5	−13.49	
20:00	1961	5.54	4.3	16.5	3.1	8.4	10.1	17.6	4.6	1.4	9.5	5.8	26.1	23.8	−13.48	0.72311
21:00	1755	5.70	4.1	16.9	3.3	8.9	10.6	19.1	4.8	1.5	9.9	6.1	28.0	23.8	−13.49	
22:00	1658	5.80	4.0	17.2	3.2	9.0	10.5	18.7	4.8	1.4	10.3	6.1	28.1	25.4	−13.60	
23:00	1539	5.67	3.9	17.9	3.5	9.5	11.1	20.5	4.9	1.6	10.6	6.5	30.5	27.2	−13.44	0.72306
24:00	1427	5.61	3.8	17.8	3.5	9.6	11.1	20.7	5.0	1.6	10.5	6.4	30.5	27.4	−13.51	
01:00	1375	5.72	3.8	18.5	3.7	10.2	11.6	22.1	5.0	1.6	10.8	6.7	35.5	28.4	−13.51	
02:00	1319	5.67	3.8	18.6	3.8	10.2	11.6	22.4	5.1	1.6	11.1	6.7	35.0	25.1	−13.56	0.72296
03:00	1274	5.49	3.8	18.4	3.6	10.1	11.6	21.4	5.2	1.6	11.2	6.7	32.4	24.8	−13.62	
04:00	1226	5.68	3.7	19.2	3.7	10.6	11.9	22.6	5.3	1.8	11.5	6.9	33.2	28.3	−13.64	
05:00	1150	5.75	3.7	20.5	3.7	10.6	11.8	22.0	5.3	1.6	11.2	6.7	34.0	29.1	−13.86	0.72313
06:00	1111	5.69	3.8	19.7	3.8	11.3	12.6	23.1	5.3	1.8	11.8	6.9	34.6	30.0	−13.61	
07:00	1041	5.76	3.9	18.8	3.7	11.1	12.5	22.8	5.4	1.9	11.7	7.0	31.1	28.8	−13.59	
2–3 June 2009																
11:30	1663	7.61	3.6	22.5	5.0	12.5	13.7	12.3	6.6	9.2	23.3	7.8	40.2	30.7	−16.38	
12:30	1744	7.62	3.6	21.9	5.4	11.7	14.2	12.8	6.7	4.7	20.9	7.6	40.5	30.7	−16.34	
13:30	1805	6.86	3.2	25.2	4.0	10.9	12.0	10.9	6.9	3.4	21.3	7.4		29.2	−16.25	
14:30	1850	6.80	2.9	20.7	3.9	10.0	11.2	11.0	6.6	2.5	19.2	7.3	32.1	28.1	−16.30	
15:30	1902	6.82	2.9	20.3	3.8	9.8	11.1	10.2	6.6	2.5	19.3	7.4	32.7	27.1	−16.37	
16:30	1926	6.68	2.7	20.0	4.1	10.7	12.0	10.4	5.4	3.5	19.7	7.0		26.7	−16.41	
17:30	1914	6.77	2.5	19.8	3.7	9.4	10.4	10.1	6.7	2.4	18.4	7.0	30.7	24.8	−16.34	
18:30	1937	6.81	2.3	19.9	4.0	9.5	10.8	10.1	5.8	2.4	18.2	6.9		28.0	−16.38	
19:30	1931	6.83	2.2	20.2	4.8	9.5	11.6	11.2	5.9	2.4	18.8	7.0	31.4	28.9	−16.45	
20:30	1926	6.59	2.1	19.5	3.6	9.2	10.2	9.7	6.1	2.5	18.7	7.2	30.1	27.6	−16.40	
21:30	1914	6.75	2.0	19.7	3.6	9.3	10.5	9.7	5.9	2.4	18.6	7.1		27.5	−16.38	
22:30	1885	6.78	2.0	20.0	3.6	9.4	10.6	9.9	6.0	3.4	19.0	7.1		29.1	−16.40	
23:30	1891	6.77	2.0	20.1	3.6	9.7	11.3	9.8	5.5	3.3	21.8	7.0	33.8	28.0	−16.44	
00:30	1845	6.55	2.0	20.3	3.7	9.7	11.1	9.9	6.8	2.8	21.3	7.2	30.2	26.6	−16.43	
01:30	1845	6.80	1.9	20.4	3.8	9.7	10.8	10.3	6.1	2.4	20.2	8.2		28.3	−16.48	
02:30	1788	6.86	1.9	20.5	3.8	9.8	11.2	10.5	5.4	3.4	19.4	7.2		28.8	−16.41	
03:30	1755	6.82	1.8	20.6	3.8	9.9	10.9	10.3	5.8	2.5	20.0	7.3	33.8	29.3	−16.46	
04:30	1728	6.60	1.7	20.7	3.9	9.6	11.1	10.7	6.1	2.7	19.8	7.7	32.3	28.7	−16.45	
05:30	1706	6.74	1.9	21.0	3.9	10.3	11.4	10.9	5.3	4.0	20.1	7.6		29.1	−16.45	
06:30	1658	6.78	2.1	21.1	4.0	9.7	11.7	11.0	6.2	2.8	20.0	8.0	31.9	27.8	−16.44	
07:30	1653	6.80	2.5	21.0	3.9	9.7	11.8	11.1	6.4	2.8	20.1	9.7	34.2	30.5	−16.43	
08:30	1600	6.76	3.0	21.2	4.0	9.8	11.8	11.3	5.5	3.3	20.2	8.0		31.0	−16.42	
09:30	1621	6.80	3.5	21.2	4.4	10.4	12.3	11.8	6.2	3.0	20.2	7.8		29.1	−16.41	
10:30	1647	6.90	3.9	21.2	4.0	9.9	11.8	11.2	6.2	3.0	19.8	7.8		29.6	−16.41	

same area reported a $^{87}Sr/^{86}Sr$ value of 0.70985 for snow (de Souza et al., 2010), which is similar to rain.

Ice is directly derived from snow and is also a 'precipitation' source of ions when it melts. The average $\delta^{18}O$ ratio of melted ice from the dead ice was -16.66 ± 0.47‰. No $^{87}Sr/^{86}Sr$ value was obtained for ice. During ice formation, solutes are excluded resulting in very low solute concentrations (Fountain, 1996).

4.3. Correction for precipitation inputs

The water chemistry in the Damma catchment is characterised by very dilute meltwaters (sum of positive charge <100 meq L^{-1}), typical of waters draining granitic lithologies (White and Blum, 1995). The dissolved load is a mixture of precipitation and weathering products, and these dilute stream waters could potentially be strongly influenced by precipitation (including glacial melt).

In order to assess the contribution of weathering to the dissolved load, external inputs need to be corrected for. This is commonly achieved by using a Cl^{-} correction which assumes that all Cl^{-} measured has originated from precipitation. However, considering only rain is insufficient in glacial catchments for the following reasons: (1) the majority of precipitation occurs as snow which has a different chemical composition compared to rain, (2) there is a seasonal cycle with increased ice melt in the summer and (3) there is a daily melt cycle where the melting of snow and ice can nearly double the discharge (Table 2). Thus, it is necessary to determine the relative contributions of rain, snow and ice melt at the relevant time intervals and measure the chemical composition of each of these water sources in order to assess the contribution of precipitation to the dissolved load. For this study, 5 snow samples, 8 rain samples and two ice samples from 2007 (Tresch, 2007) were collected. The eight rain samples were chemically different from each other (Table 1) and the element to chloride ratios did not correlate with the amount of rain which fell in the two week sampling

period. The average rain composition was used rather than the rain composition weighted with respect to precipitation volumes due to the frequent overflowing of the bottle collecting the rain. The chemical composition of snow varies during snow melt due to preferential leaching and fractionation of ions (Johannessen and Henriksen, 1978; Tsiouris et al., 1985; Williams and Melack, 1991; Marsh and Pomeroy, 1999) and this will result in a non-constant X/Cl ratio during the snow melt period. Preferential leaching effects are strong for nitrate and sulphate relative to chloride (Williams and Melack, 1991; Marsh and Pomeroy, 1999), thus the precipitation corrections for these two anions may introduce a seasonal bias. Preferential elution of cations relative to chloride is much less pronounced (Marsh and Pomeroy, 1999), thus the precipitation correction for cations will be less affected than nitrate and sulphate by this leaching process. Due to the lack of samples collected during the snow melt period we could not quantify this process further.

The percentage contributions of each of the water sources (rain, snow melt and ice melt) to the total discharge were obtained using the ALPINE3D distributed model for the 2008 hydrological year (Lehning et al. (2006) and applied to the Damma glacier catchment by Magnusson et al. (2011)). ALPINE3D is an energy-balance model which can be used to model high-resolution discharge dynamics in glacio-nival watersheds. The model takes into account the observed evolution of the snow pack during the ablation season (Farinotti et al., 2010) and local meteorological parameters. Snow melt dominated the first half of the summer and ice melt dominated at the end of the summer (Fig. 4a). With the modelled contribution of sources known for each sampling day, a weighted X/Cl ratio was calculated and the precipitation correction applied as is usual. The X/Cl ratios for each of the precipitation sources were assumed to be constant throughout the year. For Ca, the average percentage of the total annual dissolved flux derived from precipitation was 10% with a range of 2% (January) to 25% (end of summer). Since the three sites were sampled at different times of day, and a diurnal melt cycle exists, an additional correction should also be applied to take into account the diurnal change in X/Cl ratios in order that data from the different sites are directly comparable. However, the data could not be corrected to take into account the time of sampling due to incomplete discharge data from Sites E and B.

A second precipitation input correction was calculated by using the meteorology station data, which recorded the volume of precipitation reaching the forefield (Fig. 2). The precipitation volume over two weeks was multiplied by the composition of the relevant rain or snow sample (ice melt was not included in this calculation). These were then added up to give an annual input flux from precipitation, which was subtracted from annual discharge fluxes obtained from the raw data and compared with annual fluxes obtained from the chloride corrected data (Table 4). These two values show very good agreement with each other, indicating that the precipitation correction is robust. The correction is quite small because dilute snow is the dominant precipitation source to this catchment. The precipitation correction decreased absolute concentrations (Fig. 3) but did not affect overall trends in chemical ratios (Fig. 5).

4.4. Stream water chemistry

The cation abundances were typical for glacial meltwaters draining alpine glaciers (Anderson et al., 1997), with $Ca^{2+} > K^{+} \approx Na^{+} > Mg^{2+}$. Anion abundances were $HCO_3^- > NO_3^- > SO_4^{2-} > F^- \approx Cl^-$ (Table 1). Although the stream waters were dilute, significant spatial, seasonal and diurnal trends were observed in both precipitation corrected and uncorrected data (Figs. 3 and 5).

Although the three sampling sites lie within 1 km of each other and drain a common lithology, spatial differences were observed. The most pronounced spatial differences were observed in $^{87}Sr/^{86}Sr$ (Fig. 6): Site B was the most radiogenic with an average $^{87}Sr/^{86}Sr$ of 0.73024 and Site E was the least radiogenic with an average $^{87}Sr/^{86}Sr$ of 0.71838. The side stream (Site B) had more dilute major element concentrations than the main stream (Sites A and E) for the majority of samples (Fig. 3, Table 1). Spatial variation was also observed in element ratios (Fig. 5). Due to diurnal variability, part of the observed differences between sites could have been caused by sampling the sites at different times of the day (Table 1).

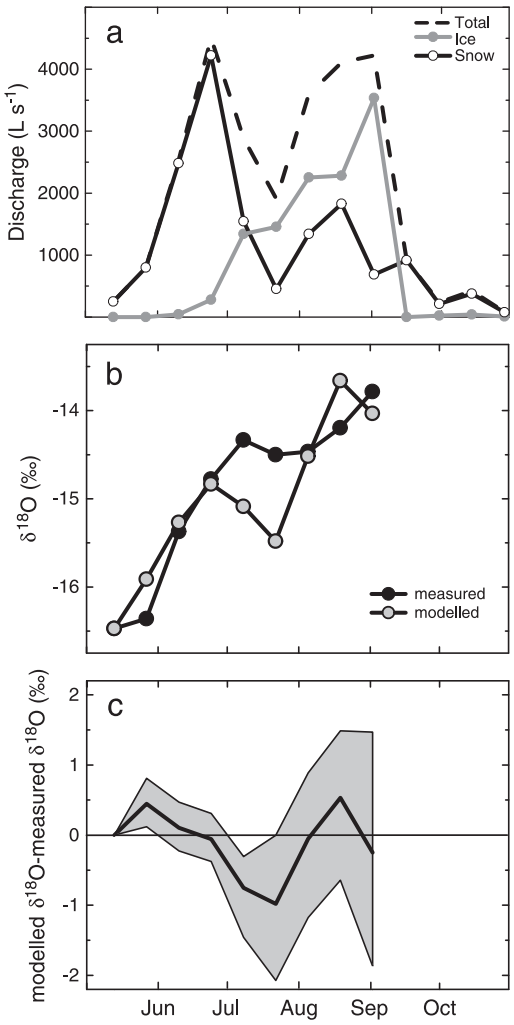

Fig. 4. (a) Proportion of snow melt and ice melt contributing to discharge on the different sampling days as modelled by ALPINE3D (Magnusson et al., 2011). (b) Comparison of modelled $\delta^{18}O$ compared to the measured values. The model is based on Rayleigh fractionation of remaining snow as the snow pack melts mixing with ice of a constant isotopic composition as described in the text. (c) The difference between modelled and measured $\delta^{18}O$. The grey area indicates the combined uncertainty of 20% in the estimation of snow and ice proportions, 10% in the estimation of catchment snow cover and 1‰ in the $\delta^{18}O$ value of ice.

The concentrations of the major elements exhibited marked seasonal and diurnal variations in response to changes in discharge (illustrated by Ca^{2+} and F^- in Fig. 3). In general, the diurnal variation of the analysed parameters was ~20% of the seasonal variation. Maximum and minimum seasonal concentrations were observed in winter and at the end of August respectively. Over a single day, maximum concentrations were observed at night and minimum concentrations were observed during mid-afternoon. Discharge varied by a factor of over 200 over the year, whereas the maximum elemental concentration variation, observed for Si, was only a factor of 10. A similar muted response of concentration variations to discharge variations was observed at the diurnal timescale and demonstrates that the variability in solute concentrations is not only controlled by dilution. The attenuated response of solutes to changes in discharge has been termed 'chemostatic' in the hydrological literature (Godsey et al., 2009; Clow

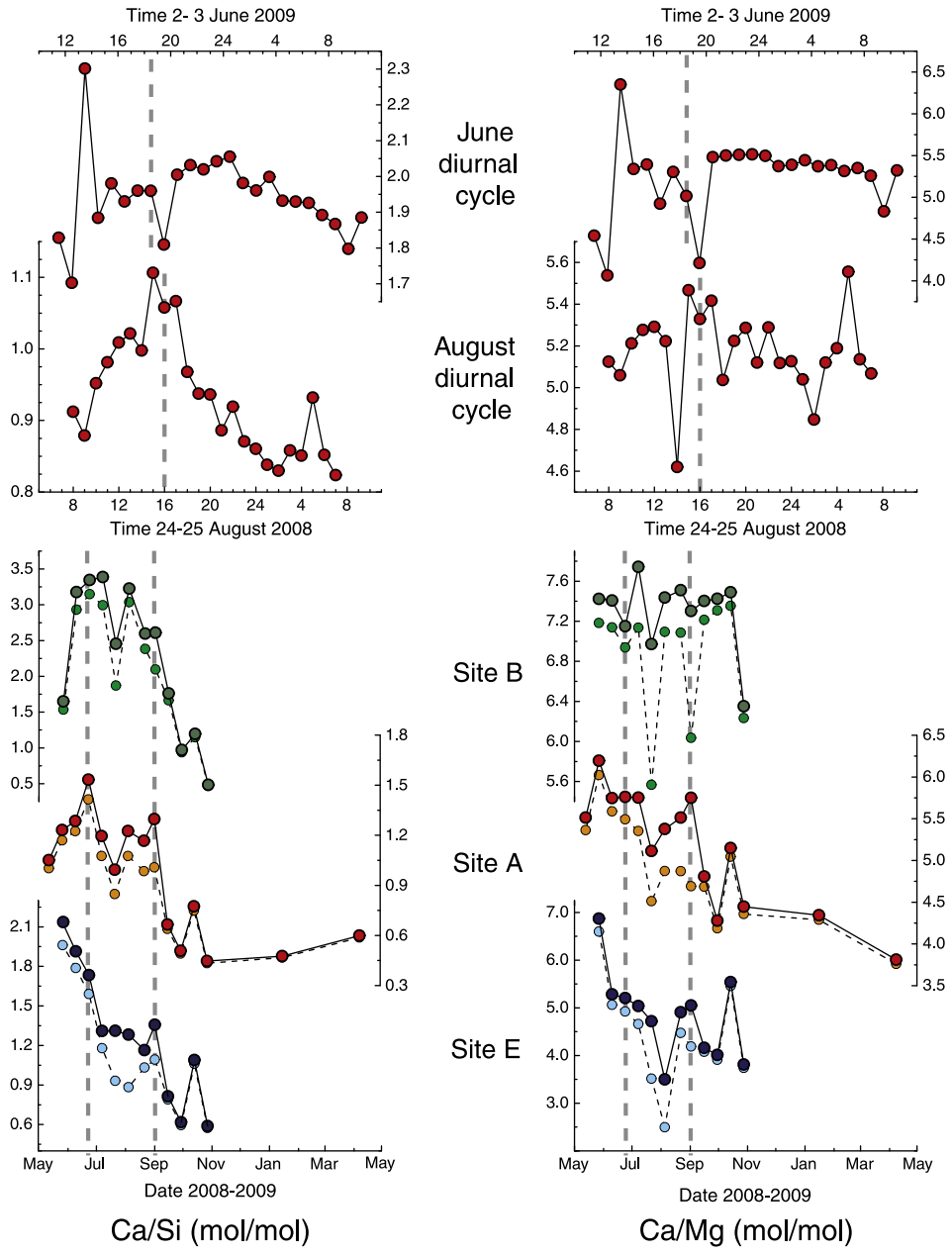

Fig. 5. Seasonal and diurnal variations in two element ratios: Ca/Si (left column) which exhibits strong temporal variability and Ca/Mg (right column) which exhibits weak temporal variability. Red symbols are data from Site A, green symbols are for Site B and blue symbols are for Site E. Precipitation corrected values are indicated by orange, light green and light blue for Sites A, B and E respectively and are joined by a dashed line. The vertical dashed lines highlight the times of maximum discharge. Average Ca/Si_{rock} was 0.06 (corrected for quartz content which is assumed not to weather) and average Ca/Mg_{rock} was 1.3 (de Souza et al., 2010).

and Mast, 2010). However, seasonal variations were observed in element ratios such as Ca/Si (Fig. 5) and such variations would not be expected if this catchment were behaving chemostatically.

At all three sites, Ca/Si ratios varied by a factor of 3–5 over the season (Fig. 5), with the lowest values observed in winter and the highest values observed during May/June when snow melt occurred. The seasonal change in Ca/Si ratios has also been observed in other glacial catchments (Hosein et al., 2004; Tipper et al., 2006; Gabet et al., 2010). Ca/Si also varied over a diurnal timescale, with the highest values coinciding with maximum discharge. The diurnal variation was most pronounced in August when the diurnal discharge amplitude was largest (2100 L s^{-1} compared to 300 L s^{-1} in June). The high concentrations of Si compared to Ca (low Ca/Si_{SiteA} ratios of 0.45–1.53) are unusual with respect to previously published data on glacial catchments (e.g. Anderson et al., 2000). Elevated Ca/Si ratios e.g. Ca/Si = 12 (Anderson et al. (2000), Bench River) are thought to be caused by calcite dissolution. The low streamwater Ca/Si ratios, together with the absence of calcite in this catchment (de Souza et al., 2010), strongly suggests that this catchment is not affected by calcite dissolution. Calcite precipitation is unlikely to occur as stream waters were always undersaturated with respect to calcite ($SI_{calcite} < -4.4$). Thus, the seasonal variation in Ca/Si ratios is unlikely to be caused by the changing proportion of carbonate to silicate weathering as proposed by Tipper et al. (2006) for Himalayan rivers.

Although a subset of element ratios exhibit similar temporal trends to Ca/Si, other element ratios exhibit different temporal responses. On a diurnal timescale Ca/Mg shows essentially invariant behaviour (Fig. 5). On a seasonal timescale there is no variation in Ca/

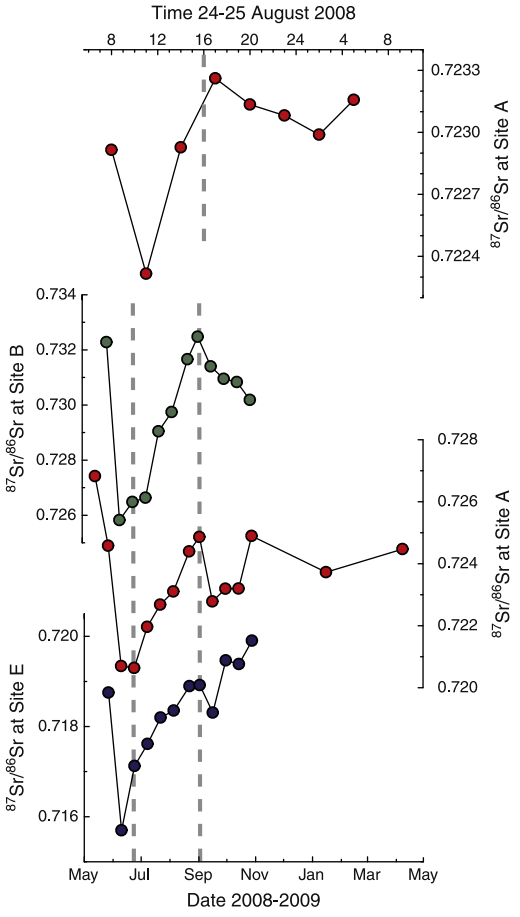

Fig. 6. Seasonal and diurnal variation in $^{87}Sr/^{86}Sr$. The dashed lines highlight the times of maximum discharge. $^{87}Sr/^{86}Sr$ decreases in response to the snow melt peak in discharge at the start of the season but does not decrease in response to high discharge later in the year. Similar variation is observed on the diurnal timescale but with a smaller magnitude. The temporal trends in $^{87}Sr/^{86}Sr$ are similar to those observed in $\delta^{18}O$ (Fig. 3).

Mg at Site B but at Site A similar variation to Ca/Si is observed. The complex and varied temporal responses of element ratios are due to different sources (e.g. preferential mineral dissolution) and processes (e.g. ion exchange, formation of secondary phases) which act on each element. In addition, element ratio variations observed at Site A could also be affected by differing relative inputs from Sites B and E.

Significant temporal variation was also observed in strontium isotopes (Fig. 6). At all three sites there was a seasonal variation in $^{87}Sr/^{86}Sr$ of 0.006, with an increase from unradiogenic values at the start of June to more radiogenic values at the end of August. After 2nd September $^{87}Sr/^{86}Sr$ at Site B decreased whereas at Site E it continued to increase. Site A reflects values which are a mixture of the isotopic fluxes at Sites B and E (discussed further in Section 5.2.1). Diurnal variation in $^{87}Sr/^{86}Sr$ in August was 0.001 with an increase in values from mid-morning to mid-afternoon. The temporal trends in $^{87}Sr/^{86}Sr$ were not related to variations in discharge or element ratios but they do appear related to the temporal trends observed for $\delta^{18}O$ (compare Figs. 3 and 6).

5. Discussion: water sources, solute sources and weathering processes

In the following discussion we will refer to water sources and chemical sources. We define *water sources* based on hydrology and $\delta^{18}O$, and *chemical sources* based on major element chemistry and $^{87}Sr/^{86}Sr$. The chemical composition of each water source can be measured at its origin, but along its flowpath its chemical composition can change and it can mix with other water sources, complicating source apportionment.

5.1. Identifying water sources

Identifying the sources of water and their flowpaths is crucial to understanding how rivers acquire their solutes (Malard et al., 1999; Brown et al., 2006), but is often neglected in many studies of chemical weathering. The ALPINE3D hydrological model (Magnusson et al., 2011) showed that snow and ice melt were the principal water components of this catchment, with the first half of the summer dominated by snow melt and the second half dominated by ice melt (Fig. 4a). Evapotranspiration and sub-surface components are minor contributors to the water budget of this catchment and can thus be neglected. Evapotranspiration contributed less than 3% of the water budget for this catchment (Kormann, 2009) and an additional sub-surface component was not required to accurately model the annual hydrograph. Variation in $\delta^{18}O$ reflects the changing hydrological properties of the catchment and the increase in $\delta^{18}O$ over the season, observed at all three sites, is typical for snow covered catchments (e.g. Bottomley et al., 1986; Unnikrishna et al., 2002; Welp et al., 2005). The $\delta^{18}O$ values of the water inputs to the catchment can be used to provide information on the temporal changes of the water source contributions to the stream and aid in the interpretation of the observed chemical changes.

The validity of the source apportionment derived from the ALPINE3D hydrological model was tested by using it to predict the $\delta^{18}O$ value of the river water, and comparing these values to the observed values. Since the response of the catchment to rain events is very rapid (cf Fig. 2) and it did not rain on any of the sampling days, rain was neglected as a water source, reducing the problem to snow and ice inputs. A snow pack is initially composed of isotopically distinct layers reflecting different precipitation events, but over time isotopic redistribution processes serve to vertically homogenise snowpack $\delta^{18}O$ values (Raben and Theakstone, 1998; Taylor et al., 2001; Unnikrishna et al., 2002). These processes occur during snow crystal metamorphism as a result of melting, freezing and vapour transport of water within the snowpack. The observation that meltwaters are isotopically lighter than the snowpack is understood to occur as a result of the fractionation of oxygen isotopes during melting, with ^{18}O preferentially retained in the ice phase (Taylor et al., 2001; Unnikrishna et al., 2002).

To estimate the $\delta^{18}O$ composition of water derived from the partial melting of snow, it is necessary to take into account the isotopic fractionation between the solid phase (snow/ice) and water. This process can be represented by a Rayleigh fractionation process, where the $\delta^{18}O$ of the meltwater at time t ($\delta^{18}O_t$) is a function of the fraction of snow remaining (f).

$$\delta^{18}O_t = \left(\delta^{18}O_0 + 1000\right) f^{\alpha_{water-ice}-1} - 1000 \quad (1)$$

The equilibrium fractionation factor between water and ice ($\alpha_{water-ice}$) was taken to be 0.9965 at 0 °C (Gat, 1996). The fraction of snow remaining in the catchment (f) was modelled by Farinotti et al. (2010) based on daily photographs of the catchment. It is assumed that on 13th May, f is 1 and thus $\delta^{18}O_0$ is taken to be −16.47‰ (Table 1). Variations in $\delta^{18}O$ can occur with altitude, with lower $\delta^{18}O$ values at higher elevations (Gat, 1996), but as no systematic variations with altitude were observed, we assumed a homogeneous snow-pack.

The isotopic composition of snow melt will be further modified by mixing with ice melt. Since the fraction of ice removed compared to the total glacial ice volume is negligible, a constant $\delta^{18}O$ for ice of

−16.66‰, based on seven melted ice samples from the dead ice block, was assumed. The estimated $\delta^{18}O$ values of snow melt and ice melt were combined according to the proportions derived from the ALPINE3D model (Magnusson et al., 2011) to estimate the bulk $\delta^{18}O$ of the river water.

$$\delta^{18}O_{river} = \delta^{18}O_{ice} \cdot F_{ice} + \delta^{18}O_{snow} \cdot F_{snow} \quad (2)$$

where F is the fractional contribution to discharge and $F_{ice} + F_{snow} = 1$.

The modelled seasonal variation of $\delta^{18}O$ in the river was compared to the measured values up to 2nd September. The predicted and observed $\delta^{18}O$ values agree remarkably well for such a simple model, with less than 1‰ discrepancy (Fig. 4b and c). This implies that the systematic increase in $\delta^{18}O$ over the season can be adequately explained by inputs from snow melt, controlled by fractional melting, mixing with ice melt. Discrepancies with the observed data could arise for a number of reasons. Firstly, there was an estimated error of 20% in the proportions of snow to ice melt from the ALPINE3D model. Secondly, the $\delta^{18}O$ value of glacier ice was not well constrained. Thirdly, rain inputs were neglected. Although it did not rain on any of the sampling days, water from previous rain events could still be percolating through the forefield. Fourthly, the Rayleigh approximation assumes the snow pack is a well-mixed, uniform reservoir; a state which is unlikely to be maintained throughout the melt season. Fifthly, during the percolation of meltwater through the snowpack and underlying ice, further isotopic exchange can occur (Taylor et al., 2001; Lee et al., 2010).

Although the retreat of the snow pack is important for the balance of snow to ice melt, it is also important to consider glacial drainage (though this will not change $\delta^{18}O$) as this will determine the contact time between water and sub-glacial sediments, potentially affecting the chemical composition of the water. The form of the hydrograph can help to infer glacial drainage. With its lower albedo, ice melts much more rapidly than snow and accentuates the daily discharge amplitude (Fountain, 1996), whereas snow cover attenuates daily discharge amplitude. The rapid melting of ice contributes to the development of a channelised (short water residence time) subglacial drainage system which also serves to accentuate the daily discharge amplitude (Nienow et al., 1996). Thus, the difference between the maximum and the minimum discharge (daily discharge amplitude) each day reflects the amount of snow cover on the glacier and the nature of the subglacial drainage system. In 2008 the daily discharge amplitude increased up to mid-September reflecting the retreat of the snow-line and thereafter abruptly decreased in response to new snow. At the start of the melt season the drainage capacity of the glacier is low due to contracted channels and the glacier cannot drain water at the same rate as it is supplied from the glacier. Drainage capacity increases as the season progresses as melt water melts the ice causing channel expansion (Schuler et al., 2004). This change in drainage can be inferred from the time difference between maximum solar insolation and maximum discharge (Fountain, 1996) and this time difference reached its minimum value at the end of August (Kormann, 2009), implying that this was when the subglacial network was draining most efficiently. These two parameters together point to an expanding channel network and decreased snow cover up until the beginning of September. Thereafter, the combination of a reducing channel network and new snow fall in mid-September caused the drainage efficiency and resulting discharge (Fig. 2) to sharply decrease. Thus, although $\delta^{18}O$ did not exhibit large variation during September (the sources remained the same), the way the water drained had changed. This sudden 'shutdown' of the glacial drainage system induced noticeable changes in the streamwater chemistry, as discussed below.

5.2. Identifying chemical sources of solutes

Whilst $\delta^{18}O$ and the ALPINE3D model show that the main water sources in this catchment are snow and ice melt, there could be additional water sources such as porewater and groundwater which are concentrated in solutes but are negligible for the total water balance. Even with only two water sources, variation in flow path length could create a number of different chemical sources through changes in the elemental composition as a result of processes such as dissolution, secondary mineral precipitation, exchange and biological cycling.

5.2.1. Sources of $^{87}Sr/^{86}Sr$

The $^{87}Sr/^{86}Sr$ ratio of the stream reflects the mixing of sources with different $^{87}Sr/^{86}Sr$ ratios, for example, different minerals or external dust inputs. However, $^{87}Sr/^{86}Sr$ should be insensitive to secondary process such as the precipitation of secondary phases. The $\delta^{18}O$ ratios of groundwater samples are similar to those of the river (Table 3) suggesting connectivity between the stream and shallow groundwater (Malard et al., 1999; Magnusson et al., submitted for publication), which could influence $^{87}Sr/^{86}Sr$. If there are no Sr inputs from the forefield areas and Sr is conservative over short timescales then Site A should fall on a mixing line between Sites E and B in $^{87}Sr/^{86}Sr$ vs 1/[Sr] space for each sample (Langmuir et al., 1978). The minimum deviation between the mixing line and Site A data points can be calculated as the perpendicular distance from the mixing line. The calculated deviation from conservative mixing is small (<1 fmol L^{-1} Sr and an average $^{87}Sr/^{86}Sr$ deviation of 0.00135‰) and shows no seasonal trend (not shown). Much of the difference can be attributed to difference in sample collection times: $^{87}Sr/^{86}Sr$ at Site A had a diurnal variation of ~0.001.

Ground and porewaters could contribute to the water mixture at Site A. However, porewaters have extremely heterogeneous chemical compositions (Table 3) and do not plot on the mixing line between sites E and B in Fig. 7. The $\delta^{18}O$ of the porewaters varied between rain values and river values suggesting that some of the porewaters were isolated with no connectivity to the stream. The groundwater sample were neither chemically nor isotopically distinct from the stream water samples (Fig. 7) and, as the volume contribution to total discharge was minor (Section 5.1), will consequently have an imperceptible effect on the stream water chemistry observed at Site A. Although we cannot completely exclude a contribution from ground and porewaters, it is likely that the forefield soils between Sites E and A have a negligible impact on the dissolved flux of Sr and this should be true for other elements which have similar chemical behaviour to Sr. Thus, for Sr, Site A can be explained as a simple mixture of waters from Sites E and B.

Previous measurements of $^{87}Sr/^{86}Sr$ in mineral separates and rocks from the catchment indicated a large degree of heterogeneity (de Souza et al., 2010). It is thus likely that differences in the degree of metamorphic resetting of radiogenic Sr are controlling the spatial difference in $^{87}Sr/^{86}Sr$ between Sites E and B rather than different weathering conditions in each of the sub-catchments. For example, in terms of $^{87}Sr/^{86}Sr$ ratios (Fig. 7), Site E appears to drain a lithology more akin to the gneissic rock sample R04 (0.71613) and the mylonitic rock sample R05 (0.75577) is more representative of Site B (Fig. 7, de Souza et al., 2010). Due to the large heterogeneity of $^{87}Sr/^{86}Sr$ in the mineral separates measured by de Souza et al. (2010) we cannot ascribe the stream water chemistry to a specific composition of minerals weathering.

Significant dust deposition, principally from Saharan dust storms (De Angelis and Gaudichet, 1991; Thevenon et al., 2009), occurs along the Alpine chain. Saharan dust contains 20–50% carbonate (Goudie and Middleton, 2001) which is dissolved during transport by atmospheric aerosols (De Angelis and Gaudichet, 1991). The addition of dissolved carbonates could impact stream water chemistry at

Table 3
Major species, $^{87}Sr/^{86}Sr$ and $\delta^{18}O$ data for groundwater (GW) and porewater (PW) samples. Measurement reproducibility is described in the text.

Sample name	Ca^{2+}	Mg^{2+}	Na^{+}	K^{+}	Si	F^{-} (μmol L^{-1})	Cl^{-}	NO_3^{-}	PO_4^{3-}	SO_4^{2-}	HCO_3^{-}	Sr^{2+} (nmol L^{-1})	$\delta^{18}O$ (‰)	$^{87}Sr/^{86}Sr$
GW1a	23.2	4.8	20.2	17.4	59.1	12.1	5.3	12.1	–	7.8	62.7	34.6	−13.11	0.72959
GW1b	59.0	5.1	17.2	15.5	39.7	15.3	94.7	7.5	–	7.7	36.2	52.1	−14.17	
GW1c	34.8	5.4	16.4	15.6	42.6							36.9		0.72831
GW2a	49.9	16.8	21.7	41.3	45.2	3.6	12.9	27.2	–	5.8		100.1	−13.96	
GW2b	41.2	9.4	22.7	23.2	53.1	9.6	1.6	4.6	–	11.4	127.8	53.5	−14.09	
GW2c	47.5	10.3	24.1	25.2	54.9	9.4	21.7	11.0	–	12.5	106.8	63.9	−14.08	
GW3a	120.5	23.7	22.4	42.6	78.1	6.3	809.4	–	–	3.6		144.8	−13.10	
GW3b	51.2	20.9	20.5	38.0	74.7	4.4	33.1	–	–	2.3	204.5	80.1	−13.27	
GW3c	42.4	19.2	18.4	38.6	62.2							75.5		0.71553
GW4b	13.7	3.0	3.9	13.0	4.3	2.4	2.3	5.4	–	3.4	29.6	21.8	−14.23	
GW5b	13.6	2.4	3.7	12.6	5.4	2.6	1.4	6.9	–	4.2	27.4	21.9	−14.12	
GW6b	14.7	5.9	9.1	19.6	25.8	8.5	1.4	6.8	–	4.2	55.4	18.1	−14.78	
PW1a	152.0	14.2	27.6	44.5	15.7	0.0	468.5	10.6	–	2.5		45.6	−18.18	
PW1b	149.3	49.6	18.8	17.6	17.2	1.7	223.4	–	–	2.1		119.3	−10.29	
PW1c	22.3	8.6	23.1	32.3	61.9	3.4	19.0	1.4		8.7	–	30.6	−12.10	0.71691
PW1d	19.7	8.5	22.4	30.2	61.5	3.3	10.2	1.7		9.0	–	30.0	−12.24	
PW1e	33.1	13.1	22.8	27.7	42.9	3.5	10.2	–	–	7.6	117.9	46.2	−13.60	
PW2a	2760.8	59.9	19.5	139.5	52.4							1114.0		0.70840
PW2b	75.3	5.8	15.8	44.2	14.9	3.3	250.2	6.5	1.9	1.7		23.2	−14.12	
PW2c	268.5	149.4	184.0	196.8	15.0	9.3	677.0	836.6	4.6	293.5		272.8	−8.72	0.71577
PW3a	37.0	6.8	1.7	15.7	26.2	4.3	96.9	0.4	–	0.8		27.2		0.71570
PW3b	59.2	15.5	18.6	29.4	9.0							59.8		0.71652
PW4	550.4	95.5	47.5	138.5	93.9	15.6	1135.8	–	–	3.3	579.3	493.6	−14.04	0.72276
PW5	591.7	8.2	51.8	26.5	20.5	0.0	3568.1	–	38.5	0.0		40.1	−19.29	
PW6	78.0	10.7	18.7	8.4	34.7	0.9	159.9	–	–	1.7		22.0	−6.42	
PW8	57.7	1.1	352.9	11.0	2.7	2.5	125.5	2.7	–	2.2		23.7	−14.21	
PW11	428.2	66.6	47.4	374.3	89.0	12.5	1304.3	11.1	–	24.9	570.8	279.8	−13.03	0.71447
PW13	3974.5	37.6	33.6	53.9	108.1	21.4	–	24.4	42.0	6.2		2753.8	−9.05	
PW21	339.7	45.0	34.8	102.5	50.3							331.2		0.71237

− Indicates species was below the detection limit.
Blank space indicates species was not measured.

Damma. However, the comparatively low Ca/Si ratios observed suggest that carbonate dust deposition does not strongly influence the stream water chemistry of this catchment.

Seasonal trends in $^{87}Sr/^{86}Sr$ have been observed in other catchments (Krishnaswami et al., 1992; Aubert et al., 2002; Tipper et al., 2006; Bélanger and Holmden, 2010), and these have been linked to discharge control of weathering sources. It was proposed that discharge controls which chemically distinct areas of a catchment (Aubert et al., 2002) and which minerals (Bullen et al., 1996; Tipper et al., 2006) contribute to the dissolved load. In this fieldsite, the lowest flows have the most radiogenic $^{87}Sr/^{86}Sr$ ratios, which is broadly consistent with previous studies (Bullen et al., 1996; Tipper et al., 2006). However, a simple discharge control cannot explain the $^{87}Sr/^{86}Sr$ data since discharge is not correlated with $^{87}Sr/^{86}Sr$ ($R^2_{SiteA} = 0.17$).

The seasonal variation in $^{87}Sr/^{86}Sr$ at Damma is identical in form to that which would be predicted by the rapid addition and subsequent depletion of an unradiogenic source (Nezat et al., 2010). We demonstrated in the previous section that $\delta^{18}O$ can be explained by the relative degree of snow and ice melt from the forefield and the glacier surface. If the 27th May sample is excluded then there is a linear relationship between $\delta^{18}O$ and $^{87}Sr/^{86}Sr$ for all sites (e.g. Site E, $R^2 = 0.62$). The correlation of $^{87}Sr/^{86}Sr$ with $\delta^{18}O$ suggests that the variations in $^{87}Sr/^{86}Sr$ can similarly be explained by snow melt. Total discharge is composed of snow melt and ice melt. We can consider that a fraction of this flow (f^*) comes into contact with sub-glacial sediment where it acquires solutes and $^{87}Sr/^{86}Sr$ ratios derived from dissolution, hereafter termed *sub-glacial* flow. Although two main types of subglacial drainage system exist (channelised and distributed, Nienow et al., 1996), we assume that the isotopic composition of strontium released from weathered sediments is unaffected by the nature of the sub-glacial drainage system. The rest of the discharge is en-glacial (within the glacier) or supra-glacial (on the glacier surface) flow where there is negligible solute acquisition. We term these last two components *surface melt*. As explained above, we assume that the groundwater and porewater inputs are negligible. The following mass balance equation can be written for Sr isotopes:

$$\phi_t[Sr]_t R_t = f^*\left(\phi_{ice}[Sr]^*_{ice}R^*_{ice} + \phi_{snow}[Sr]^*_{snow}R^*_{snow}\right) + \left(1-f^*\right)\left(\phi_{ice}[Sr]_{ice}R_{ice} + \phi_{snow}[Sr]_{snow}R_{snow}\right) \quad (3)$$

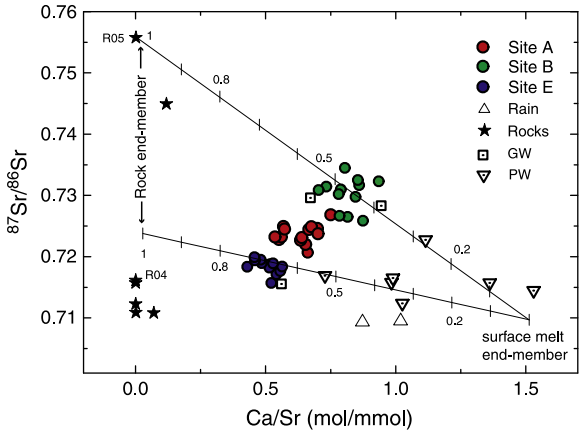

Fig. 7. Mixing plot of $^{87}Sr/^{86}Sr$ against [Ca]/[Sr]. Site E can be explained as a mixture between average rock and a surface melt component. The surface melt end-member has a Ca/Sr ratio which is an average of snow samples and a $^{87}Sr/^{86}Sr$ ratio which is the average of the rain samples (Table 1). We assume $^{87}Sr/^{86}Sr_{snow} = {}^{87}Sr/^{86}Sr_{rain}$. Similarly, Site B can be explained by mixing of the surface melt component with the most radiogenic rock sampled (R05). Site A is a mixture between Sites B and E. The numbers on the mixing lines refer to the fractional contribution from rock. Rock data are from de Souza et al. (2010). Porewaters (PW) have distinct compositions and have negligible influence on the stream water composition at Site A. Groundwater samples (GW) have identical compositions to the stream water indicating connectivity between the two (Magnusson et al., submitted for publication), though they will not influence the stream water composition at Site A.

where ϕ is the discharge, the subscript t is for 'total' and the asterisk indicates concentrations ([Sr]) and isotope ratios (R) modified by interaction with sub-glacial sediments. We assume ice has the same isotopic composition and Sr concentration as snow and the combined term is given the subscript g for 'glacial'.

$$\phi_t[\mathrm{Sr}]_t R_t = f^*\phi_t[\mathrm{Sr}]_g^* R_g^* + \left(1-f^*\right)\phi_t[\mathrm{Sr}]_g R_g \quad (4)$$

If the concentrations and isotopic compositions of the two mixing components are assumed to be constant throughout the season then the value of f^* can be determined by fitting Eq. (4) with the values of R_t, ϕ_t and $[\mathrm{Sr}]_t$ observed at Site A. The physical plausibility of the calculated values of f^* can then be assessed. The values of $[\mathrm{Sr}]_g$ and R_g are assumed to be constant with values of 2.35 nmol L^{-1} (average snow [Sr], Table 1) and 0.70971 (snow 87Sr/86Sr, from de Souza et al. (2010)) respectively. The choice of these values is supported by the fact that stream water data for Sites B and E lie on mixing lines between the surface melt end-member and rock compositions in $^{87}Sr/^{86}Sr$ vs Ca/Sr space (Fig. 7). During winter, the contribution of surface melt is expected to be negligible and these winter samples should represent the sub-glacial component. Thus, 74 nmol L^{-1} for $[\mathrm{Sr}]_g^*$ and 0.73248 for R_g^* were chosen as these were the highest values observed in the stream water during winter. The calculated amounts of sub-glacial and surface meltwater compared to the total discharge are illustrated in Fig. 8.

An independent approximation of the proportion of sub-glacial water can be obtained from the shape of the diurnal hydrograph. Diurnal discharge variations are driven by day-time melting of the glacier surface. It is assumed that the difference between the discharge at the time of sampling and the night-time minimum represents addition of surface melt which does not weather sediments ($1-f^*$). Although some of this water will inevitably reach the bed of the glacier, its effect, on a diurnal timescale, is to enlarge existing channels (Schuler et al., 2004), thus increased water–sediment contact will be minimal. Minimal melting of the glacier surface is expected to occur at night, therefore we assume that the diurnal minimum represents sub-glacial flow only (f^*). These values of f^* agree with the fitted values in the latter half of the season but underestimate the proportion of surface melt water at the start of the melt season (Fig. 8). During this part of the year, snow melt from the glacier surface dominates and maintains high flow rates even at night, due to the long time lag (>7 h) between maximum runoff and maximum solar insolation. Snow melt at night leads to an over-estimation of the amount of sub-glacial water at this time of the year.

Although further data would be needed to verify the assumptions made, to a first approximation, the fitted amounts of surface and sub-glacial meltwater are plausible based on current understanding of glacier hydrology and the strontium isotopic composition of the stream water can be explained by a two-component mixture of surface melt and subglacial water, whose composition is controlled by local lithology (Fig. 7). The relative proportions of these two solute sources are controlled by the evolution of the glacial drainage system over the melt season.

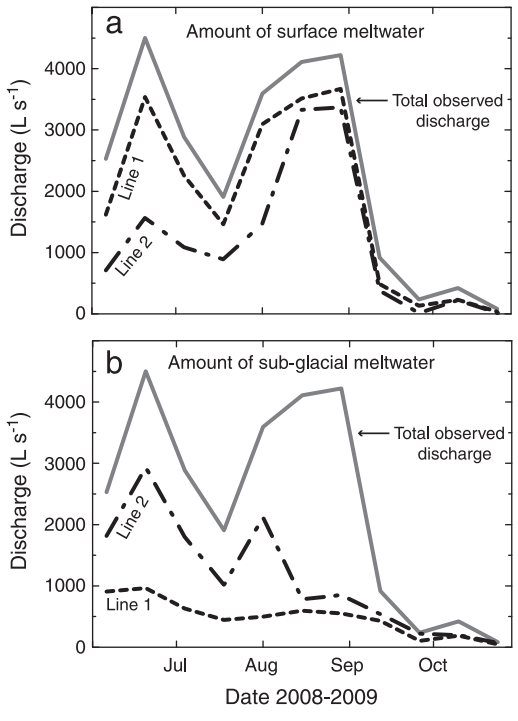

Fig. 8. The calculated amount of surface meltwater (a) and the amount of sub-glacial meltwater (b) with respect to the observed total discharge. In both figures line 1 (dotted) represents values obtained by fitting Eq. (4) to observed values, assuming fixed chemical and isotopic compositions of the two components (see text). In (a) the values of line 2 (dash-dot) are the difference between the minimum diurnal discharge and the discharge at the time of sampling, assumed to represent surface glacial melt only. The values of line 2 in (b) are the minimum discharge values observed on the sampling day, assumed to represent sub-glacial meltwater only. The discrepancy between the two sets of values at the start of the melt season is likely to be due to snow-melt causing elevated diurnal discharge minima, leading to an overestimation of the amount of water which has interacted with sub-glacial sediments.

5.2.2. Elemental sources

Elemental ratios did not correlate with Sr isotopes, which only trace chemical sources. This implies that processes (e.g. adsorption) play an important role in modulating stream water chemistry in addition to chemical sources. The diurnal changes in stream water chemistry are very similar to those observed seasonally. We thus infer that the underlying controls on stream water chemistry are the same at both the diurnal and the seasonal timescales.

There are at least three processes which could alter elemental ratios within a water body: biological cycling, weathering and ion exchange.

Biological cycling could affect elemental ratios on diurnal and seasonal timescales in response to changing nutrient requirements. However the effect of biology on stream water chemistry in this catchment is expected to be negligible due to the sparse vegetation cover and the limited influence of porewaters on stream water chemistry (Section 5.2.1). Further, stable isotope analyses of Sr and Ca have shown that the effect of biological cycling on river Sr and Ca is negligible (de Souza et al., 2010; Hindshaw et al., 2011). Weathering processes can affect element ratios by altering the ratio of ions released into solution during dissolution or through precipitation processes selectively removing ions from solution. Silicate dissolution rates vary with temperature and pH and the stream water temperature exhibited clear diurnal variation (Table 2). White et al. (1999) reported the effect of temperature on individual elemental release rates from laboratory experiments. Using the temperature–elemental release rate relationships for Ca and Si derived for the most compositionally similar granite to Damma (weathered Loch Vale granite), we can calculate that an 8 °C variation in temperature would be required to explain the observed diurnal variation in Ca/Si ratios in August. This change in temperature is much larger than the 3 °C change observed. There was no clear diurnal variation in streamwater pH, therefore the influence of pH on Ca/Si ratios is expected to be minimal. Thus, changing silicate dissolution rates are unlikely to cause diurnal variations of element ratios. Ion exchange and sorption processes have rapid kinetics (Stumm and Morgan, 1996) and are known to cause the release of base cations during flushing with dilute water i.e. snow melt (e.g. Clow and Mast, 2010). The effect of flushing with dilute water on element ratios such as Ca/Na appears to be catchment specific (Malard et al., 1999; Tranter et al., 2002; Clow and

Mast, 2010). Ion exchange is undoubtedly important in this catchment but this process was unable to be quantified further.

Rather than the chemical composition of a single water body changing, the seasonal and diurnal variations could be caused by mixing different water bodies which have different chemical compositions (Malard et al., 2000). Previous work on glacial drainage systems using dye tracers has identified two major components namely a 'distributed' component which is characterised by longer residence times and a 'channelised' component which is characterised by shorter residence times (Nienow et al., 1996; Brown, 2002). The drainage system of the Damma glacier presumably behaves in a similar way.

Waters with different residence times have the potential to acquire different solute compositions. Laboratory experiments have shown that the initial stages of weathering are incongruent, resulting in the preferential release of Ca, Mg, K and Sr relative to Si and, to a certain extent, Na (Acker and Bricker, 1992; Brantley et al., 1998; White et al., 1999). Under high discharge conditions (short residence time), the stream water chemistry is likely to reflect incongruent weathering processes, whereas water with a longer residence time is expected reflect more congruent weathering. This prediction is in agreement with other fieldsites where high cation/Si ratios are often observed in water with short residence times compared to water with long residence times (Brown et al., 2006; Tipper et al., 2006; Gabet et al., 2010). It is therefore plausible that the diurnal and seasonal variations are caused by the variable mixing of water with different residence times and chemical compositions. For elemental ratios Eq. (4) would become:

$$\phi_t X_t = af^{**}\phi_t X_g^{*ch} + (1-a)f^{**}\phi_t X_g^{*dis} + \left(1-f^{**}\right)\phi_t X_g \quad (5)$$

where $X_g^{*}{}^{ch}$ and $X_g^{*}{}^{dis}$ are the chemical ratios of the channelised (short residence time, more incongruent weathering) and distributed

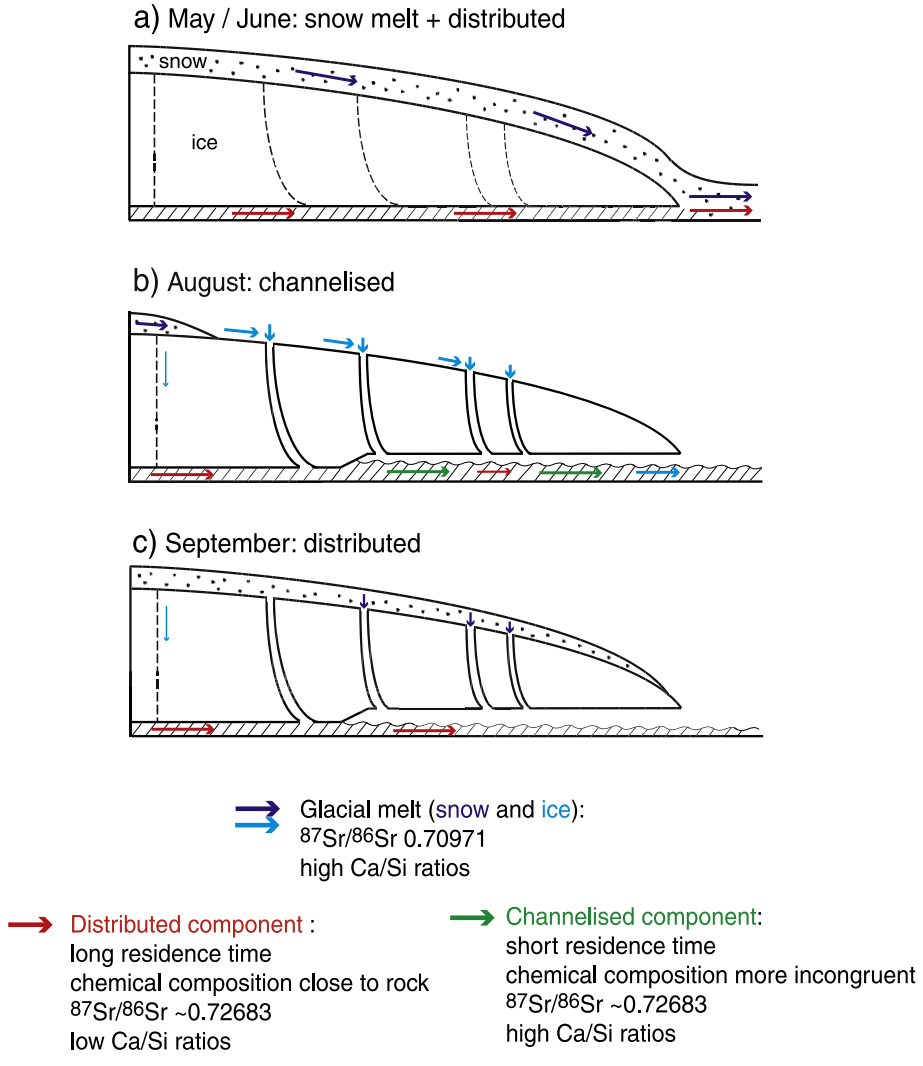

Fig. 9. Conceptual model of how the glacier hydrology controls stream water chemistry represented by three different times during the season. Figure based on Brown (2002). Blue arrows represent chemical contributions from snow and ice melt and red and green arrows represent chemical contributions from distributed and channelised sub-glacial flowpaths respectively. (a) At the beginning of the season snow still covered the glacier, but significant snow melt was occurring from the surface. This water mixed with concentrated water from the base of the glacier (distributed flow). (b) By August all snow in the ablation zone of the glacier had melted and crevasses had opened up which allowed icemelt to reach the bed of the glacier expanding sub-glacial channels and creating the fast channelised component which dominated the river chemistry. (c) In September, new snow fall which was not subject to strong melting due to cold temperatures, effectively sealed the crevasses (which gradually froze up) blocking transfer of melt water through crevasses. This resulted in a return to distributed flow conditions which persisted throughout the winter. During winter baseflow is maintained through pressure melting.

(long residence time, more congruent weathering) components respectively, a is the fraction of sub-glacial flow in the channelised system and f^{**} is the mixing proportion. With our data we cannot quantitatively constrain the fractional contributions of the channelised and distributed components but the observed changes in elemental ratios qualitatively support the mixing of waters with different residence times.

On a diurnal timescale, high meltwater discharge during mid-afternoon increases the channelised component (Stone and Clarke, 1996), resulting in high Ca/Si ratios compared to the night (Fig. 5). The Ca/Si diurnal variation is more pronounced in August compared to June due to the larger diurnal discharge amplitude. Both Ca and Mg are preferentially released during incongruent weathering (Erel et al., 2004). Hence the Ca/Mg ratio is not expected to be strongly affected by variations in residence time and remains constant on this timescale (Fig. 5).

Similarly, changes in hydrological flowpaths can explain the observed seasonal variations. The channelised component increases in proportion as the melt season progresses due to increased melt forcing the expansion and merging of smaller sub-glacial channels (Tranter et al., 1996). Thus, the channelised component is expected to dominate during summer (Fig. 9b) causing high Ca/Si ratios (Fig. 5). In autumn, colder conditions and new snow block the melting of ice and the distributed flowpaths become more prominent (Fig. 9c) as evinced by the drop in Ca/Si ratios after 2 September (Fig. 5). In spring/early summer, distributed flow is expected to dominate the sub-glacial hydrological drainage system, but significant snow melt (which contains negligible Si) from the glacier surface also occurs (Fig. 9a), resulting in high Ca/Si values during this period. Seasonal, but not diurnal, variability was observed in Ca/Mg ratios at Site A (Fig. 5). This could be due to freezing of the forefield area during winter. Freezing of water concentrates solutes and CO_2 (Hodgkins et al., 1998). High solute concentrations could cause the formation of secondary phases (Tranter, 2003) and Ca and Mg are likely to be affected differently by these conditions (Stallard and Edmond, 1983).

Glacial rivers tend to have high cation/Si ratios compared to non-glacial rivers (Anderson et al., 1997; Hodson et al., 2000), and this has been attributed to the production of small, reactive particles as a result of glacial grinding. However, seasonal variations in elemental ratios e.g. Ca/Si are not confined to small glaciated catchments but are also observed in other rivers where present-day glaciation is negligible (Cameron et al., 1995; Yang et al., 1996; Aubert et al., 2002; Millot et al., 2002; Hren et al., 2007; Gupta et al., 2011). Our data indicate that these variations are triggered by changes in discharge, which are amplified in glacial catchments.

In this lithologically homogeneous catchment significant variation was observed in elemental ratios, which are typically taken to indicate the degree of mixing between carbonate and silicate end-members (e.g. Gaillardet et al., 1999). If an increased Ca/Na ratio was taken to indicate increased carbonate weathering rather than increased incongruency in silicate weathering, then cation release, and thus CO_2 consumption, from silicate weathering would be underestimated. For example, a typical formula for calculating silicate derived cation concentrations in meq is (Galy and France-Lanord, 1999):

$$\sum cat^{*}_{sil} = \mathrm{Na}^{*} + \mathrm{K}^{*} + \left(2\mathrm{Na}^{*} \times (\mathrm{Ca}/\mathrm{Na})_{rock}\right) + \left(2\mathrm{K}^{*} \times (\mathrm{Mg}/\mathrm{K})_{rock}\right) \quad (6)$$

where the asterisk refers to precipitation corrected data. If we take the average rock molar ratios, $(Ca/Na)_{rock}$ and $(Mg/K)_{rock}$, to be 0.38 and 0.28 respectively (Hindshaw et al., 2011), and use the precipitation corrected annual fluxes from Table 4, then the calculated silicate cationic flux would be 66 meq/m^2/yr. This value is 44% less than that calculated assuming no carbonate contribution (117 meq/m^2/yr, Table 4). If this degree of underestimation applies to other rivers then our findings could have implications for current global estimates of silicate weathering rates.

Table 4
Annual elemental fluxes.

Element	Annual flux (uncorrected)	Annual flux* (kmol/km^2/yr)	Annual flux**	External contribution to annual flux* (%)
Ca	36	32	29	11
Mg	7	6	6	5
Na	21	19	18	10
K	24	21	21	12
Si	34	33	33	1
Cl	9	n.a.	8	–
F	12	11	12	5
NO_3	28	21	14	23
SO_4	13	11	8	12
HCO_3	64	n.d.	n.d.	n.d.
Total cationic flux (meq/m^2/yr)		117	108	

*Chloride method.
**Hydrological method.

6. Conclusions

The stream water chemistry in this catchment is strongly controlled by glacial melt and the routing of this glacial melt water through the glacier, resulting in marked seasonal and diurnal variations in $\delta^{18}O$, $^{87}Sr/^{86}Sr$, element concentrations and element ratios. Hydrological modelling combined with oxygen isotope data showed that the two principal water sources in this catchment were snow and ice melt. The two primary chemical sources, as identified by strontium isotopes, were surface melt (consisting of supra-glacial and en-glacial snow and ice melt) and a mineral source derived from the weathering of sub-glacial sediments. This mineral source varied in its elemental composition depending on the residence time of the water in the glacial drainage system. Fast flow paths (channelised), which are dominant in summer and during the day, are characterised by high cation/Si ratios. Whereas slow flow paths (distributed), which are dominant in winter and at night, are characterised by low cation/Si ratios. The change in residence time could potentially influence several weathering related processes. Thus, the primary control on cation/Si ratios is the water flux and the pathway of that water through the glacier.

Our results emphasise that even in a notionally mono-lithological catchment, there is considerable spatial heterogeneity. The hydrologic control of temporal variability observed in this study is not confined to glacial catchments, suggesting that the primary impact of glaciers on stream water chemistry is through the modulation of discharge. The hydrological conditions at the time of sampling have to be taken into account when 1) comparing rivers sampled at different flow stages, 2) calculating annual chemical weathering fluxes based on a few spot samples and 3) deriving contributions of silicate weathering. Future stream sampling campaigns should consider sampling at various spatial and temporal resolutions in order to capture the sources of change and to further increase understanding of chemical weathering processes in riverine environments.

Acknowledgements

The authors gratefully thank everyone who helped during all the water sampling trips, with special thanks to Martin Theiler for assistance during the June 24-hour sampling trip. We also thank Bruno Fritschi, Karl Steiner, Franz Herzog and Tobias Jonas for setting up and maintaining the water gauging and meteorology stations, Daniel Farinotti for providing snow cover data, Gregory de Souza for discussions, Iso Christl for setting up the IC measurements and Maria Coray Strasser for measuring $\delta^{18}O$. We thank the editor Joel D. Blum and two anonymous reviewers for their detailed comments on this

manuscript. This work was funded by the BigLink project of the ETH Competence Center Environment and Sustainability of the ETH Domain (CCES) and by ETH Research Grant No. 04/06-3.

References

Acker, J.G., Bricker, O.P., 1992. The influence of pH on biotite dissolution and alteration kinetics at low temperature. Geochim. Cosmochim. Acta 56, 3073–3092.

Anderson, S.P., Drever, J.I., Humphrey, N.F., 1997. Chemical weathering in glacial environments. Geology 25, 399–402.

Anderson, S.P., Drever, J.I., Frost, C.D., Holden, P., 2000. Chemical weathering in the foreland of a retreating glacier. Geochim. Cosmochim. Acta 64, 1173–1189.

Arn, K., Hosein, R., Föllmi, K.B., Steinmann, P., Aubert, A., Kramers, J., 2003. Strontium isotope systematics in two glaciated crystalline catchments: Rhone and Oberaar glaciers (Swiss Alps). Schweiz. Mineral. Petrogr. Mitt. 83, 273–283.

Aubert, D., Probst, A., Stille, P., Viville, D., 2002. Evidence of hydrological control of Sr behavior in stream water (Strengbach catchment, Vosges mountains, France). Appl. Geochem. 17, 285–300.

Bélanger, N., Holmden, C., 2010. Influence of landscape on the apportionment of Ca nutrition in a Boreal Shield forest of Saskatchewan (Canada) using $^{87}Sr/^{86}Sr$ as a tracer. Can. J. Soil Sci. 90, 267–288.

Bernasconi, S.M., Christl, I., Hajdas, I., Zimmermann, S., Hagedorn, F., Smittenberg, R., Furrer, G., Zeyer, J., Brunner, I., Frey, B., Plötze, M., Lapanje, A., Edwards, P., Olde Venterink, H., Göransson, H., Frossard, E., Bünemann, E., Jansa, J., Tamburini, F., Welc, M., Mitchell, E., Bourdon, B., Kretzschmar, R., Reynolds, B., Lemarchand, E., Wiederhold, J., Tipper, E., Kiczka, M., Hindshaw, R., Stähli, M., Jonas, T., Magnusson, J., Bauder, A., Farinotti, D., Huss, M., Wacker, L., Abbaspour, K., 2008. Weathering, soil formation and initial ecosystem evolution on a glacier forefield: a case study from the Damma Glacier, Switzerland. Miner. Mag. 72, 19–22.

Berner, R.A., Rao, J.-L., Chang, S., O'Brien, R., Keller, C.K., 1998. Seasonal variability of adsorption and exchange equilibria in soil waters. Aquat. Geochem. 4, 273–290.

Bullen, T.D., Krabbenhoft, D.P., Kendall, C., 1996. Kinetic and mineralogic controls on the evolution of groundwater chemistry and $^{87}Sr/^{86}Sr$ in a sandy silicate aquifer, northern Wisconsin, USA. Geochim. Cosmochim. Acta 60, 1807–1821.

Bluth, G.J.S., Kump, L.R., 1994. Lithologic and climatologic controls of river chemistry. Geochim. Cosmochim. Acta 58, 2341–2359.

Bottomley, D.J., Craig, D., Johnston, L.M., 1986. Oxygen-18 studies of snowmelt runoff in a small precambrian shield watershed: implications for streamwater acidification in acid-sensitive terrain. J. Hydrol. 88, 213–234.

Brantley, S.L., Chesley, J.T., Stillings, L.L., 1998. Isotopic ratios and release rates of strontium measured from weathering feldspars. Geochim. Cosmochim. Acta 62, 1493–1500.

Brown, G.H., 2002. Glacier meltwater hydrochemistry. Appl. Geochem. 17, 855–883.

Brown, L.E., Hannah, D.M., Milner, A.M., Soulsby, C., Hodson, A.J., Brewer, M.J., 2006. Water source dynamics in a glacierized alpine river basin (Taillon-Gabiétous, French Pyrénées). Water Resour. Res. 42, W08404.

Buttle, J.M., 1994. Isotope hydrograph separations and rapid delivery of pre-event water from drainage basins. Prog. Phys. Geog. 18, 16–41.

Cameron, E.M., Hall, G.E.M., Veizer, J., Krouse, H.R., 1995. Isotopic and elemental hydrogeochemistry of a major river system: Fraser River, British Columbia, Canada. Chem. Geol. 122, 149–169.

Clow, D.W., Drever, J.I., 1996. Weathering rates as a function of flow through an alpine soil. Chem. Geol. 132, 131–141.

Clow, D.W., Mast, M.A., 2010. Mechanisms for chemostatic behavior in catchments: implications for CO_2 consumption by mineral weathering. Chem. Geol. 269, 40–51.

De Angelis, M., Gaudichet, A., 1991. Saharan dust deposition over Mont Blanc (French Alps) during the last 30 years. Tellus 43B, 61–75.

de Souza, G.F., Reynolds, B.C., Kiczka, M., Bourdon, B., 2010. Evidence for mass-dependent isotopic fractionation of strontium in a glaciated granitic watershed. Geochim. Cosmochim. Acta 74, 2596–2614.

Dempster, T.J., 1986. Isotope systematics in minerals: biotite rejuvenation and exchange during Alpine metamorphism. Earth Planet. Sci. Lett. 78, 355–367.

Deniel, C., Pin, C., 2001. Single-stage method for the simultaneous isolation of lead and strontium from silicate samples for isotopic measurements. Anal. Chim. Acta 426, 95–103.

Erel, Y., Blum, J.D., Roueff, E., Ganor, J., 2004. Lead and strontium isotopes as monitors of experimental granitoid mineral dissolution. Geochim. Cosmochim. Acta 68, 4649–4663.

Fairchild, I.J., Killawee, J.A., Sharp, M.J., Spiro, B., Hubbard, B., Lorrain, R.D., Tison, J.-L., 1999. Solute generation and transfer from a chemically reactive alpine glacial-proglacial system. Earth Surf. Process. Landforms 24, 1189–1211.

Farinotti, D., Magnusson, J., Huss, M., Bauder, A., 2010. Snow accumulation distribution inferred from time-lapse photography and simple modelling. Hydrol. Process. 24, 2087–2097.

Fountain, A.G., 1996. Effect of snow and firn hydrology on the physical and chemical characteristics of glaical runoff. Hydrol. Process. 10, 509–521.

France-Lanord, C., Evans, M., Hurtrez, J.-E., Riotte, J., 2003. Annual dissolved fluxes from Central Nepal rivers: budget of chemical erosion in the Himalayas. C. R. Geosci. 335, 1131–1140.

Gabet, E.J., Wolff-Boenisch, D., Langner, H., Burbank, D., Putkonen, J., 2010. Geomorphic and climatic controls on chemical weathing in the High Himalayas of Nepal. Geomorphology 122, 205–210.

Gaillardet, J., Dupré, B., Louvat, P., Allègre, C.J., 1999. Gobal silicate weathering and CO_2 consumption rates deduced from the chemistry of large rivers. Chem. Geol. 159, 3–30.

Galy, A., France-Lanord, C., 1999. Weathering processes in the Ganges-Brahmaputra basin and the riverine alkalinity budget. Chem. Geol. 159, 31–60.

Garrels, R.M., Mackenzie, F.T., 1967. Origin of the chemical compositions of some springs and lakes. In: Gould, R.F. (Ed.), Equilibrium Concepts in Natural Water Systems. : Advances in Chemistry Series, vol. 67. American Chemical Society, Washington DC, pp. 222–242.

Gat, J.R., 1996. Oxygen and hydrogen isotopes in the hydrologic cycle. Annu. Rev. Earth Planet. Sci. 24, 225–262.

Gíslason, S.R., Arnórsson, S., Ármannsson, H., 1996. Chemical weathering of basalt in southwest Iceland: effects of runoff, age of rocks and vegetative/glacial cover. Am. J. Sci. 296, 837–907.

Godsey, S.E., Kirchner, J.W., Clow, D.W., 2009. Concentration-discharge relationships reflect chemostatic characteristics of US catchments. Hydrol. Process. 23, 1844–1864.

Goudie, A.S., Middleton, N.J., 2001. Saharan dust storms: nature and consequences. Earth Sci. Rev. 56, 179–204.

Gupta, H., Chakrapani, G.J., Selvaraj, K., Kao, S.-J., 2011. The fluvial geochemistry, contributions of silicate, carbonate and saline-alkaline components to chemical weathering flux and controlling parameters: Narmada River (Deccan Traps), India. Geochim. Cosmochim. Acta 75, 800–824.

Hindshaw, R.S., Reynolds, B.C., Wiederhold, J.G., Kretzschmar, R., Bourdon, B., 2011. Calcium isotopes in a proglacial weathering environment: Damma glacier, Switzerland. Geochim. Cosmochim. Acta 75, 106–118.

Hodgkins, R., Tranter, M., Dowdeswell, J.A., 1998. The hydrochemistry of runoff from a 'cold-based' glacier in the High Arctic (Scott Turnerbreen, Svalbard). Hydrol. Process. 12, 87–103.

Hodson, A., Tranter, M., Vatne, G., 2000. Contemporary rates of chemical denudation and atmospheric CO_2 sequestration in glacier basins: an Arctic perspective. Earth Surf. Process. Landforms 25, 1447–1471.

Hosein, R., Arn, K., Steinmann, P., Adatte, T., Föllmi, K.B., 2004. Carbonate and silicate weathering in two presently glaciated, crystalline catchments in the Swiss Alps. Geochim. Cosmochim. Acta 68, 1021–1033.

Hren, M.T., Chamberlain, C.P., Hilley, G.E., Blisniuk, P.M., Bookhagen, B., 2007. Major ion chemistry of the Yarlung Tsangpo-Brahmaputra river: Chemical weathering, erosion, and CO_2 consumption in the southern Tibetan plateau and eastern syntaxis of the Himalaya. Geochim. Cosmochim. Acta 71, 2907–2935.

Jobard, S., Dzikowski, M., 2006. Evolution of glacial flow and drainage during the ablation season. J. Hydrol. 330, 663–671.

Johannessen, M., Henriksen, A., 1978. Chemistry of snow meltwater: changes in concentration during melting. Water Resour. Res. 14, 615–619.

Kormann, C., 2009. Untersuchungen des Wasserhaushaltes und der Abflussdynamik eines Gletschervorfeldes. Master's thesis, TU Dresden.

Krishnaswami, S., Trivedi, J.R., Sarin, M.M., Ramesh, R., Sharma, K.K., 1992. Strontium isotopes and rubidium in the Ganga - Brahmaputra river system: Weathering in the Himalaya, fluxes to the Bay of Bengal and contributions to the evolution of oceanic $^{87}Sr/^{86}Sr$. Earth Planet. Sci. Lett. 109, 243–253.

Langmuir, C.H., Vocke, R.D., Hanson, G.N., Hart, S.R., 1978. A general mixing equation with applications to Icelandic basalts. Earth Planet. Sci. Lett. 37, 380–392.

Lee, J., Feng, X., Faiia, A.M., Posmentier, E.S., Kirchner, J.W., Osterhuber, R., Taylor, S., 2010. Isotopic evolution of a seasonal snowcover and its melt by isotopic exchange between liquid water and ice. Chem. Geol. 270, 126–134.

Lehning, M., Völksch, I., Gustafsson, D., Nguyen, T.A., Stähli, M., Zappa, M., 2006. ALPINE3D: a detailed model of mountain surface processes and its application to snow hydrology. Hydrol. Process. 20, 2111–2128.

Likens, G.E., Driscoll, C.T., Buso, D.C., Siccama, T.G., Johnson, C.E., Lovett, G.M., Fahey, T.J., Reiners, W.A., Ryan, D.F., Martin, C.W., Bailey, S.W., 1998. The biogeochemistry of calcium at Hubbard Brook. Biogeochemistry 41, 89–173.

Liu, F., Williams, M.W., Caine, N., 2004. Source waters and flow paths in an alpine catchment, Colorado Front Range, United States. Water Resour. Res. 40, W09401.

Magnusson, J., Farinotti, D., Jonas, T., Bavay, M., 2011. Quantitative evaluation of different hydrological modelling approaches in a partly glacierized Swiss watershed. Hydrol. Process. doi:10.1002/hyp.7958.

Magnusson, J., Kobierska, F., Huxol, S., Jonas, T., Kirchner, J.W., submitted for publication. Melt water driven stream and groundwater stage fluctuations on a glacier forefield (Damma gletscher, Switzerland). Hydrol. Process.

Malard, F., Tockner, K., Ward, J.V., 1999. Shifting dominance of subcatchment water sources and flow paths in a glacial floodplain, Val Roseg, Switzerland. Arct. Antarct. Alp. Res. 31, 135–150.

Malard, F., Tockner, K., Ward, J.V., 2000. Physico-chemical heterogeneity in a glacial riverscape. Landscape Ecol. 15, 679–695.

Marsh, P., Pomeroy, J.W., 1999. Spatial and temporal variations in snowmelt runoff chemistry, Northwest Territories, Canada. Water Resour. Res. 35, 1559–1567.

Meybeck, M., 2003. Global occurrence of major elements in rivers. In: Holland, H.D., Turekian, K.K. (Eds.), Treatise on Geochemistry. : Surface and ground water, weathering and soils, vol. 5. Elsevier.

Millot, R., Gaillardet, J., Dupré, B., Allègre, C.J., 2002. The global control of silicate weathering rates and the coupling with physical erosion: new insights from rivers of the Canadian Shield. Earth Planet. Sci. Lett. 196, 83–98.

Mitchell, A.C., Brown, G.H., Fuge, R., 2001. Minor and trace element export from a glacierized Alpine headwater catchment (Haut Glacier d'Arolla, Switzerland). Hydrol. Process. 15, 3499–3524.

Nezat, C.A., Blum, J.D., Driscoll, C.T., 2010. Patterns of Ca/Sr and $^{87}Sr/^{86}Sr$ variation before and after a whole watershed $CaSiO_3$ addition at the Hubbard Brook Experimental Forest, USA. Geochim. Cosmochim. Acta 74, 3129–3142.

Nienow, P.W., Sharp, M., Willis, I.C., 1996. Velocity-discharge relationships derived from dye tracer experiments in glacial meltwaters: implications for subglacial flow conditions. Hydrol. Process. 10, 1411–1426.

Oliva, P., Viers, J., Dupré, B., 2003. Chemical weathering in granitic environments. Chem. Geol. 202, 225–256.
Ollivier, P., Hamelin, B., Radakovitch, O., 2010. Seasonal variations of physical and chemical erosion: a three-year survey of the Rhone River, (France). Geochim. Cosmochim. Acta 74, 907–927.
Raben, P., Theakstone, W.H., 1998. Changes in ionic and oxygen isotopic composition of the snowpack at the glacier Austre Okstindbreen, Norway, 1995. Nord. Hydrol. 29, 1–20.
Reeder, S.W., Hitchon, B., Levinson, A.A., 1972. Hydrogeochemistry of the surface waters of the Mackenzie River drainage basin, Canada — I. factors controlling inorganic composition. Geochim. Cosmochim. Acta 36, 825–865.
Riebe, C.S., Kirchner, J.W., Finkel, R.C., 2004. Erosional and climatic effects on long-term chemical weathering rates in granitic landscapes spanning diverse climate regimes. Earth Planet. Sci. Lett. 224, 547–562.
Schaltegger, U., 1994. Unravelling the pre-Mesozoic history of Aar and Gotthard massifs (Central Alps) by isotopic dating — a review. Schweiz. Miner. Petrog. Mitt. 74, 41–51.
Schuler, T., Fischer, U.H., Gudmundsson, G.H., 2004. Diurnal variability of subglacial drainage conditions as revealed by tracer experiments. J. Geophys. Res. 109, F02008.
Sharp, M., Tranter, M., Brown, G.H., Skidmore, M., 1995. Rates of chemical denudation and CO_2 drawdown in a glacier-covered alpine catchment. Geology 23, 61–64.
Shiller, A.M., 1997. Dissolved trace elements in the Mississippi River: seasonal, interannual, and decadal variability. Geochim. Cosmochim. Acta 61, 4321–4330.
Stallard, R.F., Edmond, J.M., 1983. Geochemistry of the Amazon 2. The influence of geology and weathering environment on the dissolved load. J. Geophys. Res. 88, 9671–9688.
Stone, D.B., Clarke, G.K.C., 1996. *In situ* measurements of basal water quality and pressure as an indicator of the character of subglacial drainage systems. Hydrol. Process. 10, 615–628.
Stumm, W., Morgan, J.J., 1996. Aquatic Chemistry: Chemical Equilibria and Rates in Natural Waters, 3rd ed. Wiley.
Taylor, S., Feng, X., Kirchner, J.W., Osterhuber, R., Klaue, B., Renshaw, C.E., 2001. Isotopic evolution of a seasonal snowpack and its melt. Water Resour. Res. 37, 759–769.
Thevenon, F., Anselmetti, F.S., Bernasconi, S.M., Schwikowski, M., 2009. Mineral dust and elemental black carbon records from an Alpine ice core (Colle Gnifetti glacier) over the last millennium. J. Geophys. Res. 114, D17102.
Tipper, E.T., Bickle, M.J., Galy, A., West, A.J., Pomiès, C., Chapman, H.J., 2006. The short term climatic sensitivity of carbonate and silicate weathering fluxes: insight from seasonal variations in river chemistry. Geochim. Cosmochim. Acta 70, 2737–2754.
Tranter, M., 2003. Geochemical weathering in glacial and proglacial environments. In: Holland, H.D., Turekian, K.K. (Eds.), Treatise on Geochemistry. : Surface and ground water, weathering and soils, vol. 5. Elsevier.
Tranter, M., Brown, G.H., Hodson, A.J., Gurnell, A.M., 1996. Hydrochemistry as an indicator of subglacial drainage system structure: a comparison of alpine and sub-polar environments. Hydrol. Process. 10, 541–556.
Tranter, M., Sharp, M.J., Lamb, H.R., Brown, G.H., Hubbard, B.P., Willis, I.C., 2002. Geochemical weathering at the bed of Haut Glacier d'Arolla, Switzerland — a new model. Hydrol. Process. 16, 959–993.
Tresch, E., 2007. Hydrochemistry of the Damma glacier forefield — temporal and spatial variability. Master's thesis, ETH Zurich. http://e-collection.ethbib.ethz.ch/view/eth:30215.
Tsiouris, S., Vincent, C.E., Davies, T.D., Brimblecombe, P., 1985. The elution of ions through field and laboratory snowpacks. Ann. Glaciol. 7, 196–201.
Unnikrishna, P.V., McDonnell, J.J., Kendall, C., 2002. Isotope variations in a Sierra Nevada snowpack and their relation to meltwater. J. Hydrol. 260, 38–57.
VAW, 2005. Gletscherberichte (1881–2002) 'Die Gletscher der Schweizer Alpen', Jahrbücher der Glaziologischen Kommission der Schweizerischen Akademie der Naturwissenschaften (SANW) Versuchsanstalt für Wasserbau, Hydrologie und Glaziologie (VAW) No. 1–122. http://glaciology.ethz.ch/swiss-glaciers. ETH Zürich.
Viviroli, D., Weingartner, R., 2004. The hydrological significance of mountains: from regional to global scale. Hydrol. Earth Syst. Sci. 8, 1016–1029.
Welp, L.R., Randerson, J.T., Finlay, J.C., Davydov, S.P., Zimova, G.M., Davydova, A.I., Zimov, S.A., 2005. A high-resolution time series of oxygen isotopes from the Kolyma River: implications for the seasonal dynamics of discharge and basin-scale water use. Geophys. Res. Lett. 32, L14401.
West, A.J., Galy, A., Bickle, M., 2005. Tectonic and climatic controls on silicate weathering. Earth Planet. Sci. Lett. 235, 211–228.
White, A.F., Blum, A.E., 1995. Effects of climate on chemical weathering in watersheds. Geochim. Cosmochim. Acta 59, 1729–1747.
White, A.F., Blum, A.E., Bullen, T.D., Vivit, D.V., Schulz, M., Fitzpatrick, J., 1999. The effect of temperature on experimental and natural chemical weathering rates of granitoid rocks. Geochim. Cosmochim. Acta 63, 3277–3291.
Williams, M.W., Melack, J.M., 1991. Solute chemistry of snowmelt and runoff in an alpine basin, Sierra Nevada. Water Resour. Res. 27, 1575–1588.
Yang, C., Telmer, K., Veizer, J., 1996. Chemical dynamics of the "St. Lawrence" riverine system: δD_{H_2O}, $\delta^{18}O_{H_2O}$, $\delta^{13}C_{DIC}$, $\delta^{34}S_{sulfate}$, and dissolved $^{87}Sr/^{86}Sr$. Geochim. Cosmochim. Acta 60, 851–866.
Yde, J.C., Knudsen, N.T., Nielsen, O.B., 2005. Glacier hydrochemistry, solute provenance, and chemical denudation at a surge-type glacier in Kuannersuit Kuussuat, Disko Island, West Greenland. J. Hydrol. 300, 172–187.
Zakharova, E.A., Pokrovsky, O.S., Dupré, B., Zaslavskaya, M.B., 2005. Chemical weathering of silicate rocks in Aldan Shield and Baikal Uplift: insights from long-term seasonal measurements of solute fluxes in rivers. Chem. Geol. 214, 223–248.